Master in Artificial Intelligence

Master of Science Thesis

Looking for neuroimaging biomarkers in Huntington Disease

Author:
Daniel Padilla Carrasco

Supervisor:
Ruth de Diego Balaguer

Cosupervisor:
Estela Càmara Mancha

Facultat d'Informàtica de Barcelona (FIB)
Facultat de Matemàtiques (UB)
Escola Tcnica Superior dEnginyeria (URV)

Universitat Politècnica de Catalunya (UPC)
Universitat de Barcelona (UB)
Universitat Rovira i Virgili (URV)

Defense date: April 30, 2015

April 2015

ABSTRACT

Objective: Huntington's Disease (HD), a devastating neurogenetic disorder, is clinically diagnosed by the presence of motor symptoms. However, cognitive deficits are present before motor symptoms appear. A large body of literature has shown the involvement of the fronto-striatal and fronto-parietal circuits in cognitive control. This study aims to investigate the role of the fronto-striatal circuit as a biomarker of the deficits in executive functions observed in HD.

Methods: Twenty-six healthy adults and twenty-six HD patients underwent a functional magnetic resonance imaging involving a switching task. Two different approaches were applied: the standard general linear model and support vector machines, in order to investigate potential alterations of the fronto-striatal circuit engaged in cognitive control.

Results: Using the general lineal model, we observed a gradually decreasing activity of the fronto-striatal circuits, following the disease progression. Additionally, different support vector machines based on the fronto-striatal activation pattern have allowed us to classify participants between controls and patients, although with an accuracy level lower than expected.

RESUM

Objectiu: La malaltia de Huntington s un desordre neurogenètic devastador, diagnosticat clnicament amb la presència de smptomes motors. Tanmateix, abans que apareguin els smptomes motors ja hi han deficiències cognitives. Gran part de la literatura ja ha mostrat la implicaci dels circuits frontoestriats i frontoparietals en el control cognitiu. Aquest estudi busca investigar el paper del circuit frontoestriat com a biomarcador dels dèficits en les funcions executives observades en la malaltia de Huntington.

Mètodes: Vint-i-sis adults saludables i vint-i-sis pacients de la malaltia de Huntington es van sometre a una resonància magnètica funcional que implica una tasca de conmutaci. S'han utilitzat dos estratègies diferents: un *general linear model* i *support vector machines* per poder investigar alteracions potencials en el circuit frontoestriat encarregat en el control cognitiu.

Resultats: Utilitzant el *general linear model* observem una baixada gradual d'activaci en els circuits fronto estriats conforme la malaltia avana. Adicionalment, diferent *support vector machines* basada en l'activaci dels circuits frontoestriats han permès classificar els participants entre controls i pacients, encara que amb un percentatge d'encerts ms baix de l'esperat.

RESUMEN

Objetivo: La enfermedad de Huntington es un desorden neurogentico devastador, diagnosticado clnicamente con la presencia de sntomas motores. Sin embargo, antes de que aparezcan los sntomas motors ya hay deficiencias cognitivas. Gran parte de la literatura ya ha mostrado la implicacin de los circuitos frontoestriados y frontoparietales en el control cognitivo. Este estudio busca investigar el papel del circuito frontoestriado como biomarcador de los dficits en las funciones ejecutivas observadas en la enfermedad de Huntington.

Mtodos: Veintisis adultos saludables y veintisis pacientes de la enfermedad de Huntington se sometieron a una resonncia magntica funcional que implica una tarea de conmutacin. Se han utilitzado dos estrategias diferentes: un *general linear model* y *support vector machines* para poder investigar alteraciones potenciales en el circuito frontoestriado encargado en el control cognitivo.

Resultados: Utilizando el *general linear model* observamos una disminucin gradual de la activacin en los circuiots frontoestriados conforme la enfermedad avanza. Adems, diferentes *support vector machines* basadas en la activacin de los circuitos frontoestriados han permitido clasificar a los participantes entre controles i pacientes, aunque con un porcentage de aciertos ms bajo de lo esperado.

ACKNOWLEDGEMENTS

I would like to thank my supervisor and cosupervisor, Ruth de Diego Balaguer and Estela Càmara Mancha, for his support, for the trust placed in me with this great opportunity, and for being always there since the beginning.

Also, a special thanks to Clara Garca Gorro to help me whenever I needed help in neuroscience field topics and his general support.

A special thanks to all my family, friends and the Idibell HD group, who have given me support all this time.

Finally, I want to thank all the patients suffering from Huntington's disease and allows the investigation continue through participation.

CONTENTS

LIST OF FIGURES

LIST OF TABLES

LIST OF SOURCES

ACRONYMS

UB Universitat de Barcelona

UPC Universitat Politcnica de Catalunya

URV Universitat Rovira i Virgili

AI Artificial Intelligence

LDA Linear Discriminant Analysis

MAI Master in Artificial Intelligence

SVM Support Vector Machine

HD Huntington Disease

ROI Region of Interest

UHDRS Unified Huntington Disease Rating scale

WCST Wisconsin Card Sorting Test

Part I

PRESENTATION OF THE PROJECT

1

INTRODUCTION

Huntington's Disease (HD) [32] is a progressive neurodegenerative disease characterised by a mixture of motor, cognitive and psychiatric symptoms, which is caused by an expanded cytosine adenine guanine (CAG) repeat in exon 1 of the huntingtin gene.

Unlike other non-genetic neurodegenerative diseases as Alzheimer's Disease [21] and Parkinson's Disease [22], HD has the potential to be identified by predictive genetic testing, thereby HD being a model for studying neurodegenerative diseases before clinical onset.

This possibility of being a neurodegenerative model is what makes HD a comparatively well studied disease[1], despite being a rare disease [26] [2].

Although HD is diagnosed by the the presence of motor symptoms, cognitive and psychiatric abnomalities can be detected before motor deficits. From now on, patients who have not yet been clinically diagnosed by motor sympthoms but who will develop the disease will be refered as PreHD patients.

In this regard, many studies have shown that HD patients have cognitive deficits in executive function, which have been related to an abnormal dysfunction. For example, a study uses functional Magnetic Resonance Images (fMRI) to characterized the relationship between PreFrontal Cortex (PFC) and cognition on HD patients [9]. Another study [10] correlates the PFC with cognition (i.e, working memory) using structural Magnetic Resonance Images (MRI) on preHD patients, finding a reduction in PFC activity as the disease progress. There are also behavioural studies showing cognitive deficits in PreHD patients [12].

One of the methods for image acquisition in neuroscience is fMRI [2], which produces a brain activity map in which allows comparing

1 Searching on Google scholar: there are only 3.5 times more cites to Parkinson's Disease and 4.5 times more cites to Alzheimer's Disease than those to HD, even if Parkinson's and Alzeimer's Disease are much more prevalent.

2 Huntington prevalence is quite low, affecting to only 0,007% Europeans and even lower rates on other continents

those regions that are significantly more active when two conditions are compared.

The standard method to analyze data from these brain imaging techniques involves a General Linear Model (GLM). Th GLM is used to retrieve a brain activity map using a voxel-by-voxel regression model. This method, based on a voxel-by-voxel approach, computes the likelihood of one particular voxel to be active during a specified condition. After this step, a statistical test for rejecting the null hypothesis is used to detect any significance difference between two different conditions. The activation patterns observed in this statistical test can be related to signs of cognitive decline in the brain even before the symptoms appear. However, this univariate (voxel-by-voxel) approach makes the voxels independent on the neighbouring voxels, losing potential information that could be useful.

Even if GLM can be considered a particular case of a machine learning technique, other machine learning techniques have been used for several purposes, like classifying whether a subject is a patient or a control, or using several modalities at a time (i.e. PET & fMRI & examination results) or predicting a biomarker through regression using a multimodal approach. On this same line, this study [28] uses machine learning techniques to evaluate biomarkers for neurodegeneration in presymptomatic Huntington's Disease patients.

In the last years, the number of studies applying machine learning techniques has been increasing. One of the reasons for that fMRI involves data with high dimensionality, which can be efficiently analyzed with machine learning techniques. [19] reveal the incrementing use of machine learning techniques and the most popular classifiers: K-Means, Fisher Linear Discriminant Analysis(FLDA) and Support Vector Machines (SVM) [29] [31]. But the quantity of different machine learning techniques being applied to studies on Neuroscience field is very large. Some examples of machine learning techniques are:

K-MEANS Is a clustering method that classifies a new data point using the distance to the cluster mean.

FLDA This method extracts the linear combination of features that best explains the separation between classes.

SVM Constructs a hyperplane to separate two different classes using the bests data points to minimize the error.

GAUSSIAN PROCESSES Every single data point is associated to a Gaussian distribution variable.

RANDOM FOREST This is an ensemble method of decission trees. Decission trees is a colletion of conditions ordered by the information gain.

DEEP LEARNING A complex architecture of complex networks to classify using the extraction of abstract features.

COMPLEX NETWORKS Consisting of modelling a network to observe some particular behaviours of that model.

For example, SVM has been one of the most popular machine learning techniques applied to fMRI [24]. There are plenty of studies with SVM on different diseases like Major Depressive Disorder [20], Dementia [14], Autism [1], Multiple Sclerosis [33] or Alzheimer's Disease [15]. There is literature about SVM even on more general neurodegenerative processes; see for instance [34], which makes a study classifying the existence of a neurodegenerative disease by simple gait information. But there are also other techniques being applied and tested on neurodegenerative diseases. For example see a study on Gaussian processes classification in Alzheimer's Disease [35] and a study on the connectomics of the neurodegenerative disease using complex networks [6].

Machine learning techniques can also be found in several studies on HD. There are some examples: from a study about classification with HD carriers using only structural MRI on SVM technique [13] to detect cognitive deficits. Another study using Random Forests correlates cortical and striatal morphometry with cognitive impairments in PreHD [10], or a study with deep learning techniques using only structural MRI to classify between controls and Patients [25].

This project aims to study the neurobiological bases related to the cognitive deficits observed in the progression of HD. More concretely, MRI techniques are going to be used to identify functional biomarkers that allow, at neurophysiological level, studying the cognitive evolution of HD. By combining different MRI analysis techniques like GLM and classifiers, it will be possible to define the main neuronal circuits affected by this disease. This study could shed some light to the neurodegenerative processes in general and leading the search of a more customised medicine for those patients.

This document is structured so that the reader can follow the work done in this master thesis. Because several procedures has been performed in GLM and machine learning, the document is structured as follows:

The document starts, after this introductory chapter, with Chapter 4 where it is defined information about the Idibell HD project, a bigger project which this Thesis belongs to. Chapter 5 is to introduce the software used on this Thesis.

After that information about this project context and tools, the document follows up with the more conventional analysis part, detailed in Chapter 6, where a review of the firts steps to observe the data

statistics is done. The next chapter, Chapter 7, is about GLM and its internal procedures. Chapter 8 goes next with all the processings and the work done by the student in GLM.

The Thesis continues with the machine learning part on Chapter 9, describing Pronto sofware and a simple architecture presented to compare results with Pronto software. Similar to the conventional analysis part, Chapter 10 discuss both machine learning solutions.

On the last chapter, Chapter 11, conclusions and possible works is discussed.

2

HYPOTHESES

The main hypothesis of this Thesis is that it is possible to detect and quantify the neurophysiological deviations in cognitive control observed in HD, by means different fMRI approaches. Using a Wisconsin Sorting Card Test (WCST) task, we expect to find alterations in the fronto-striatal control circuit, due to the initial degeneration of its caudate part. More specifically, it is expected that:

1. Alteration in cognition should be initially reflected in the DLPFC region, which projects to the caudate head.
2. Classical GLM analysis will allow identifying the cognitive control circuits and distinguish between different degrees of HD progression (i.e. controls, PreHD, HD).
3. Machine learning analysis, through a multimodal approach, will allow to predict the patient proximity to the symptomatic development.

3

GOALS

The main goal of this Thesis is the identification of functional biomarkers in cognitive control for HD which allow the characterisation of the neurodegenerative process.

The specific goals are:

1. Characterisation of fronto-striatal circuit involved in the executive control function.
2. Identification of biomarkers that characterise HD the progression.
3. Development of a multimodal approach that includes information of individual differences of functional activity, correlating with neuropsychological variables related to HD patients.
4. These biomarkers should be able to predict the symptomatology development of those patients that have not yet developed any clinical symptoms.

4

CONTEXT

The problem seen in HD patients is that every one is treated as a HD patient but, when observing them individually, it can be suspected that some patients have more acute degeneration in motor control whereas other patient is more prone to have depressions and anxiety (thus, being the behavioral areas more affected). From this hypothesis, the Idibell HD project born with the aim to be able to detect these different profiles within HD patients. If these profiles can be detected, this could mean a great advance in several aspect for this disease.

Detecting these profiles could be important in order to detect which brain areas are more affected in one profile and on another, understanding why and how this HD develops on time and getting more information about this HD and, possibly, other neurodegenerative diseases.

This profile identification could also have a direct impact on HD patients, leading to different possible actions to improve the life quality of HD patients:

TREATMENT The first and most direct application could be to adapt the drugs to every profile, resulting in a more accurate and precise treatment for HD patients.

FOLLOWING A better tracing of the patient, observing the different development speed of the different profiles.

PREDICTION Forecasting the development of the disease more accurately, thus giving proper aids and scheduling to the patient.

4.1 PARTICIPANTS

Twenty-six controls and twenty-six HD patients (10 pre-Hd and 16 HD patients) participated in this study. The selection of the HD patients was done based on their Total Functional Capacity Scores (TFC), TFC $\geq$ 11 and UHDRS-motor $<$5. HD patients did not present any neurological disorders beside the HD. Participant demographics are

detailed in Table 1. Informed written consent was obtained from all participants.

	Controls	PreHD	HD
N	26	10	16
Female %	46	100	50
Age	50,13 ± 9,46	37,89 ± 10,83	49,07 ± 8,75
CAG	-	44,22 ± 2,86	44,33 ± 3,70
YTO	-	6,60 ± 12,26	-
TFC	-	12,89 ± 0,33	11,79 ± 1,31
UHDRSm	-	1,89 ± 3,33	20,47 ± 9,42
UHDRS-c	-	299,63 ± 59,71	191,14 ± 49,35
PBA-Depression	-	6,11 ± 7,47	2,06 ± 2,35
PBA-Irritability	-	3,67 ± 5,66	3,69 ± 4,88
PBA-Psycosis	-	0,56 ± 1,33	0,06 ± 0,25
PBA-Apathy	-	5,11 ± 5,93	3,81 ± 3,64
PBA-Exec.Disf.	-	4,89 ± 6,55	3,19 ± 3,60
PBA-Total	-	20,33 ± 24,46	12,81 ± 10,10

Table 1: Demographic and clinical characteristics of all participants- Mean (standard deviation) reported unless otherwise stated

(*CAG*)Cytosine-Adenine-Guanine repetitions, (*YTO*) Years to Onset, (*TFC*) Total Functional Capacity, (*UHDRSm*) Unified Huntington Disease Score Motor, (*UHDRSc*) Unified Huntington Disease Score Cognitive, (*PBA*) Problem Behaviours Assessment score,(*Exec.Disf.*)Executive Disfunction

4.2 MRI ACQUISITION

FMRI data were collected using a 3T whole-body MRI scanner (General ElectricMR750 GEM E). Tasks were back-projected onto a screen inside one virtual helmet. Magnet-compatible response buttons were used. Conventional high-resolution structural images [magnetization-prepared rapid-acquisition gradient echo sequence, repetition time (TR) 4.7 ms, echo time (TE) 4.8 ms, inversion time 450 ms, flip angle 12, 1 mm thickness (isotropic voxels)] were followed by functional images sensitive to blood oxygenation level-dependent contrast (echo planar T2*-weighted gradient echo sequence, TR=2000 ms, TE 35 ms, flip angle 90). Wisconsin task consisted of 306 sequential whole-brain volumes, comprising 30 axial slices aligned to the plane intersecting the anterior and posterior commissures, 3.5 mm in-plane resolution, 4 mm thickness, no gap, positioned to cover all but the most superior region of the brain and the cerebellum.

4.3 COGNITIVE CONTROL CIRCUIT: THE SHIFTING TASK

In the present study we used a modified version of the Monchi's task [17] in order to characterise the fronto-striatal circuit involved when performing a set shift. More concretely, it is used an adaptation from Montreal Card Sorting Test [27] to compare two conditions with different cognitive control levels. On the screen, 4 cards are presented on top and 1 card on the bottom so the subject has to match the bottom card with the top card that qualifies with the cue given at the beginning of each trial (i.e. "Colour", "Shape", "Number"). These trials are grouped in blocks of 12 consecutive trials that last for 66 seconds. These blocks can be of the different conditions. In one of the conditions, the cue will be constantly changing ("Switch" condition), in another, the condition follows always the same rule ("No Switch" condition), the last is a control condition where the subjects must match the bottom card with the identical top card ("Identity" condition). After every block there is a resting block of 20 seconds.

The total duration of this task is 13 minutes.

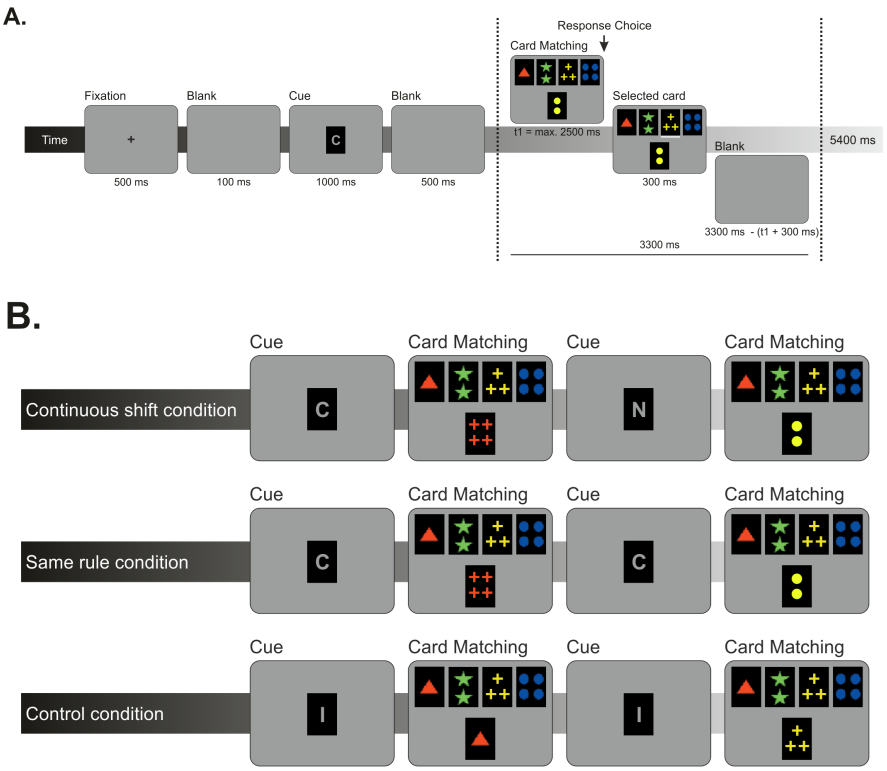

Figure 1: WCST task design

(*A*) Sequence of stimulus and response events in the fixed Wisconsin Card Sorting Test
(*B*) Task structure (12 trials for block):

- Switch condition (3 blocks)
- No switch condition (3 blocks)
- Identity condition (3 blocks)

5

RESOURCES

5.1 MATLAB

The statistical parametric mapping tool used to analyse data on this work is based on Matlab. This convert MATLAB and Statistics Toolbox Release 2012b, The MathWorks, Inc., Natick, Massachusetts, United States, in the main and only language programming in this Master Thesis.

For ML part, it will be also use the statistical toolbox of Matlab for some methods.

5.1.1 *SPM*

Statistical parametric mapping (SPM, Wellcome Department of Imaging Neuroscience, University College, London, UK, `www.fil.ion.ucl.ac.uk/spm/`) is a standard software in neuroscience for data analysis. And the fact that this Master thesis is a part of a started greater project (that was already using SPM) makes a normal choice to select Matlab as the main programming language.

It is used not only on fMRI, but also in other brain images techniques like PET or EEG. In fact, SPM comes with a GUI that allows the user to select the modality used. These modalities are "**PET & VBM**", "**M/EEG**" and "**fMRI**".

SPM offers a complete package to process the images step by step and get a final result being an activation brain map. There are also a lot of other toolbox based on SPM that allows and help the user with those aspects SPM can not do.

Although the newest is version number 12, Idibell HD projectstarted before the release of version 12. Because there are some compatibility issues between version 8 and 12, this project will use also version 8.

A more detailed explanation about software operation will be explained in sections 7.1 and 7.2.

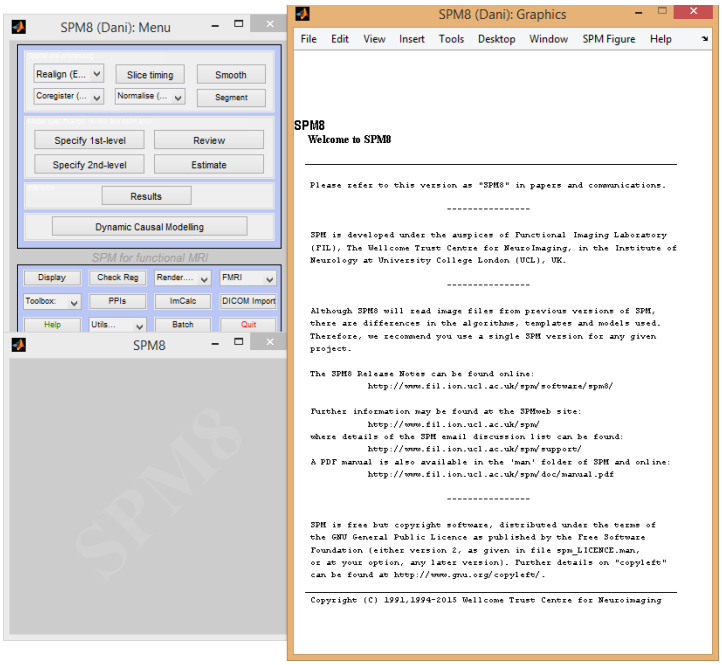

Figure 2: SPM in fMRI mode

5.1.2 *ArtRepair*

ArtRepair Software (Stanford Psychiatry Neuroimaging Laboratory `http://cibsr.stanford.edu/tools/human-brain-project/artrepair-software.html`) is an external SPM extension used to correct or discard those images with too much movement. Even though SPM comes with a movement correction, this newer toolbox is prepared for patients with high problems in motor control functions, where sudden head movements are expected.

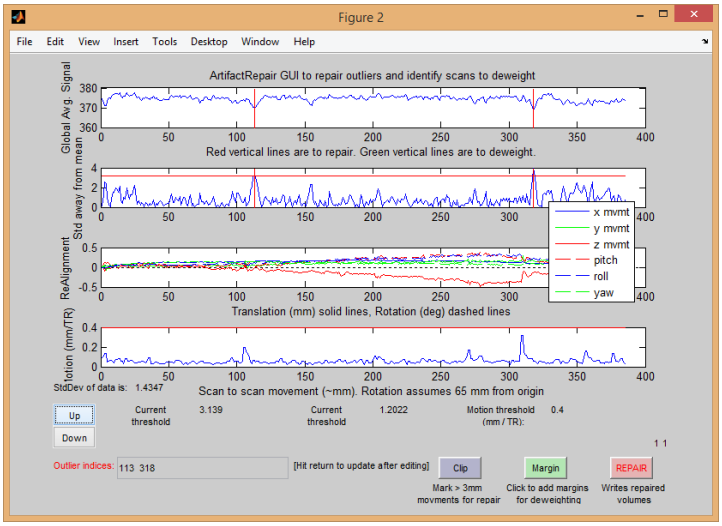

Figure 3: ArtRepair screenshot

Although it has an automatic mode, for this particular experiment it was considered better to control those images to be discarded. The desired target was to discard only two consecutive images. When images are discarded, an interpolated image is replaced, so when deleting a third consecutive image means that there is an image that has no neighbour image to interpolate with. The interpolation is made between the neighbour of its neighbour image.

This toolbox is compatible with matlabbatch.

5.1.3 *xjview*

For image and results analysis, Xjview(`whttp://www.alivelearn.net/xjview`) was used most of the time. It has some enhanced features than SPM's default viewer:

- The threshold of p-value can be changed instantly. This allow the researcher to observe the significancy of the custers by lowering or rising the p-value threshold.
- Automatic inclusion of different canonical images of the brain to localise and visualise activation clusters.

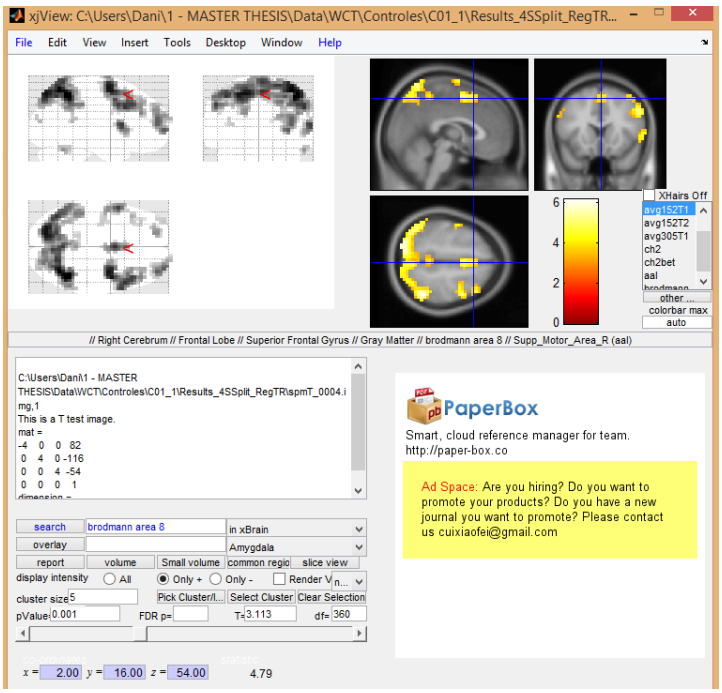

Figure 4: Xjview screenshot

5.1.4 *MarsBar*

This toolbox is a ROI toolbox for SPM. This software allows several functions with ROIs. Whereas MarsBar[4] is used as a simple ROI creator in the Thesis, it has much more options like operations with ROIs, ROI analysis, data extraction, etc.

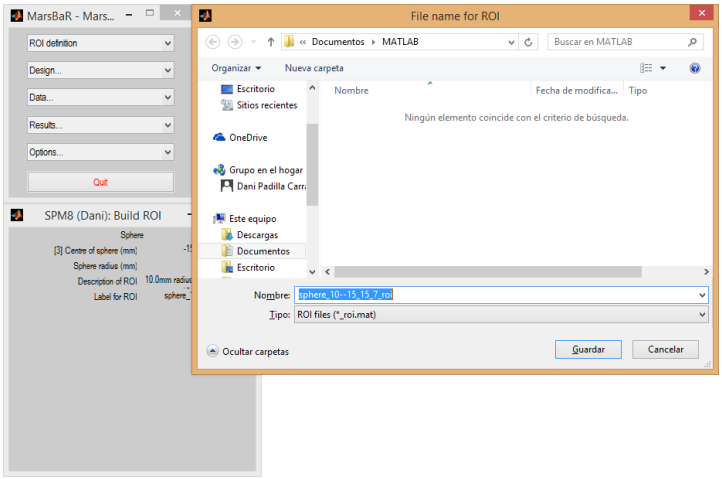

Figure 5: MarsBar operation

5.1.5 *Matlabbatch*

Surely the most used SPM extension. Although it is listed as an extension and it is a project apart, the basic SPM includes this toolbox incorporated. With it, batch scripts can be done so a single step can be automated for a large number of runs. The matlabbatch(`http://sourceforge.net/projects/matlabbatch/`) structure allows, to run batch script not only of SPM original functions but, if any extension allows it, it can be also used.

This is a great advancement: without it, considering a "large" number of subject would be a large task, since all the steps should be done manually. Considering the number of steps per subject ad the number of subjects, this will be a non-profit time-consuming task.

Source 5.1: Matlabbatch of slice timing

```
matlabbatch{1}.spm.temporal.st.scans ={files};
matlabbatch{1}.spm.temporal.st.nslices = 30;
matlabbatch{1}.spm.temporal.st.tr = 2;
matlabbatch{1}.spm.temporal.st.ta = 1.93333333333333;
matlabbatch{1}.spm.temporal.st.so = [2 4 6 8 10 12 14 ...
                                     6 18 20 22 24 26 ...
                                     28 30 1 3 5 7 9 ...
                                     11 13 15 17 19 ...
```

```
                                        21  23  25  27  29];
matlabbatch{1}.spm.temporal.st.refslice = 1;
matlabbatch{1}.spm.temporal.st.prefix = 'a';

spm_jobman('run',matlabbatch);
```

This matlabbatch script (Source 5.1) can be run several times changing the files variable so the process can be automated.

5.1.6 *WFU Pickatlas*

WFU Pickatlas[16] extension is a piece of software that allows to extract biological-based ROIs in just a few clicks. Although we do not use this software very often, it is used once in a while to get the general area that is going to be used to get the activation peak. This way we can get sphere ROIs for each subject centered in an activation peak that pertains to a biologic-specified area.

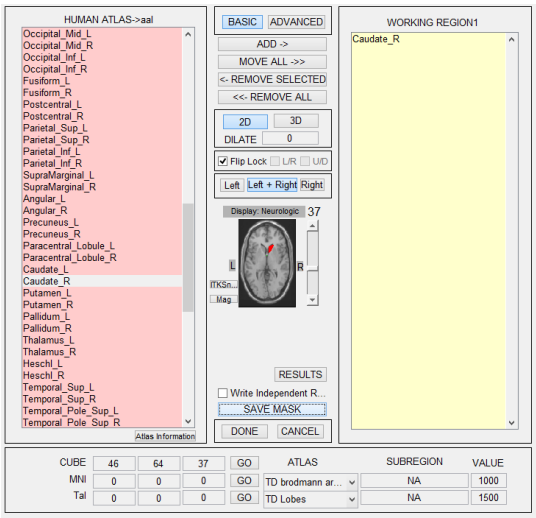

Figure 6: WFU pickatlas screenshot

5.1.7 *Pronto*

Pronto[30] stands for Pattern Recognition for Neuroimaging Toolbox and it is a software dedicated to machine learning in neuroscience. This toolbox allows the user to use a multivariate pattern recognition to face neuroimaging problems.

The toolbox, in its first version yet, allows to apply classification and regression methods to neuroimaging data using few algorithms.

This software will be explained with more details in Section 9.1.

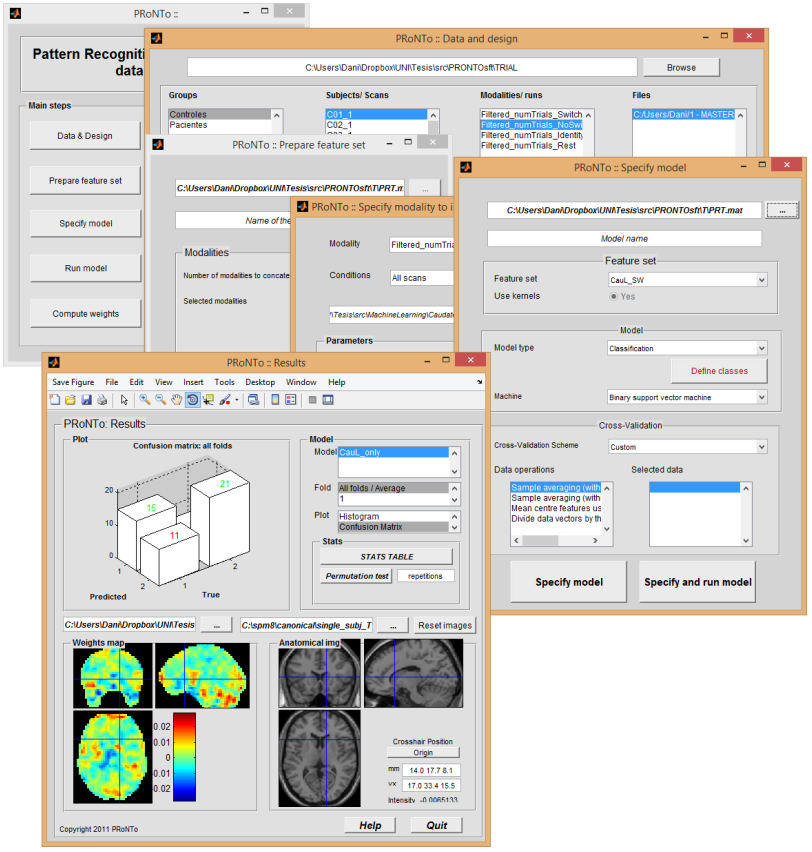

Figure 7: Pronto windows sample

This toolbox is also compatible with matlabbatch.

5.1.8 *CVX*

CVX is a package for specifying and solving convex programs[8][7].

The use of this package is to implement SVM code. As it is a convex problem, the use of this program allows the user a language specific for convex solving.

5.1.9 *LDA*

On the student approach part of the thesis it will be used some linear discriminant analysis for feature extraction. In order to ease that part, a specific LDA package[5] has been used.

5.2 SPSS

SPSS[11] is a statistical tool to analyse any dataset with a large quantity of known methods. This software has many ways to analyse the data and visualize it. Thus, is a perfect tool to have a first glance of the data hanlded.

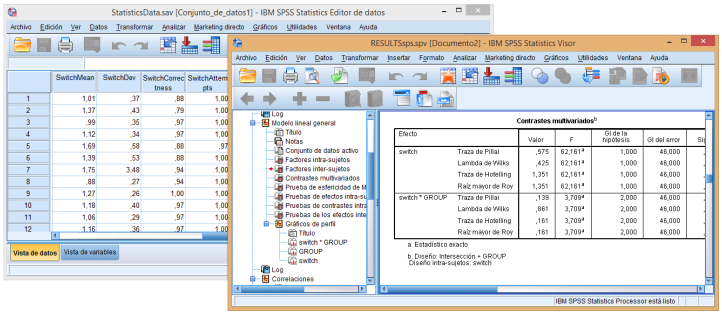

Figure 8: SPSS screenshot

As it is discussed the conductual data analysis in section 6, more information about it will be shown.

Part II

CONVENTIONAL ANALYSIS

6

BEHAVIORAL DATA

Behavioral data were analyzed using SPSS 19.0 for Windows.

Thirty-one HD patients (10 pre-HD; 16 HD) and 26 controls complete the task.

Overall, both HD patients and controls showed faster and more correct responses for the Identity condition (Reaction Time: 1.021 $\pm$ 0.34s and 97.7 $\pm$ 0.3%; Percentage of Correct Responses) compared to the Switch Condition (Reaction Time: 1.52 $\pm$ 0.49s and 87.6 $\pm$ 16.9%; Percentage of Correct Responses).

For both Reaction Time and Correct Responses, a repeated-measures ANOVA analysis was performed introducing the Switch-Cost effect (Identity condition and Switch condition) as within-factor and the group (HD, pre-HD and control) as between-subject factor.

Overall, a significant main effect of Switch was observed for the RT and the percentage of correct responses (Reaction Time: F(1,46)=262.1, $p > 0.001$; Percentage Responses: F(1,46)=24.1, $p > 0.001$, see Table 2). In particular, both HD patients and controls showed faster and more correct responses for the Identity condition (Reaction Time: 1.021 $\pm$ 0.34s and 97.7 $\pm$ 0.3%; Percentage of Correct Responses) compared to the Switch Condition (Reaction Time: 1.52 $\pm$ 0.49s and 87.6 $\pm$ 16.9%; Percentage of Correct Responses).

Moreover, a significant Switch x Group Interaction (Reaction Time: F(2,46)=13.4, $p > 0.001$; Percentage of Correct Responses: F(2,46)=6.4, $p < 0.004$) was obtained. The interaction reflects the fact that HD patients showed larger differences (for reaction times and the number of correct responses) in the Switch condition than in the Identity condition, between HD patients and controls.

While no significant differences were observed between pre-HD and controls in any of the conditions, further pairwise t-test showed significant differences between HD patients and controls for all conditions (Reaction Times: Identity t(37)=5.6,$p > 0.001$, Switch t(37)=7.8,$p > 0.001$; Percentage Correct Responses: Identity t(37))=2.7,$p < 0.01$, Switch t(37),$p > 0.001$). Pairwise t-test between pre-HD and HD

patients revealed a significant difference for reaction times (Identity: t(24)=2.8, $p > 0.01$, Switch: t(24)=4.3, $p > 0.001$) and in the percentage of correct responses for the Switch condition (t(24)=2.44, $p < 0.02$).

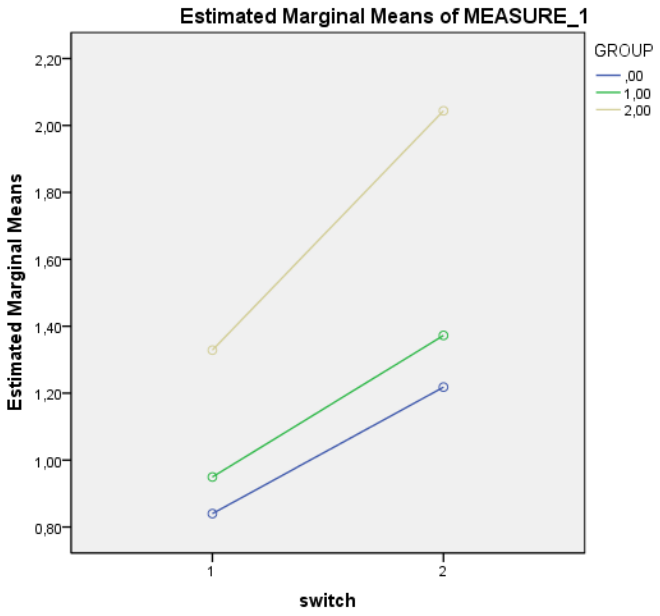

Figure 9: Mean reaction times(seconds) for each condition and group

(Legend) 0-Control, 1-PreHD, 2-HD, *(x- Axis information)* 1-Identity trials, 2-Switch trials.

	Controls	Pre-HD	HD
Identity	0.84 ± 0.14	0.95 ± 0.24	1.3 ± 0.38
Switch	1.22 ± 0.28	1.37 ± 0.39	2.04 ± 0.38

Table 2: Mean reaction times (seconds) for each condition and group

	Controls	Pre-HD	HD
Identity	0.99 ± 0.02	0.98 ± 0.02	0.96 ± 0.04
Switch	0.93 ± 0.06	0.93 ± 0.07	0.76 ± 0.21

Table 3: Mean percentage of correct responses for each condition and group

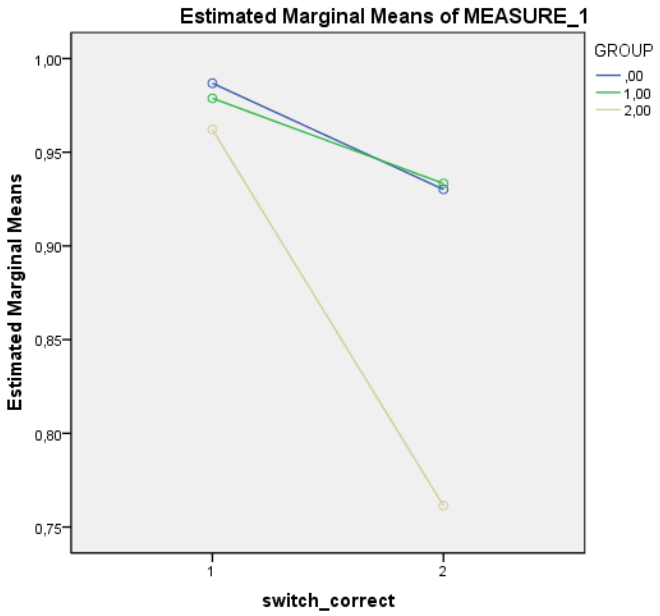

Figure 10: Mean percentage of correct responses for each condition and group

(Legend) 0-Control, 1-PreHD, 2-HD, *(x- Axis information)* 1-Identity trials, 2-Switch trials.

7

FMRI ANALYSIS

7.1 PREPROCESSING

Once the images have been acquired, they must be prepared for the analysis. This preprocessing requires several steps.

7.1.1 *Slice Timing*

MRI scanners works in slice mode so, for just one volume of 2 seconds, it has to scan, slice per slice, the whole brain. Because this process it can not be done in parallel, they must scan one slice at a time.

There are several modes in which the images can be retrieved (i.e. ascending, descending and interleaved). The scanner is set to work in an interleaved slice mode(slice 0, slice 2, slice 4... slice 1, slice 3, slice 5...).

This preprocessing step attempts to correct these little time deviations from slice to slice by applying a delaying function to the slices corresponding to its temporal position.

7.1.2 *Realignment*

After having the temporal preprocessing, we need to process the images in the spatial dimension.

The time-series that correspond to the subject is not static and every image has tiny movements. Because of these subtle (and not so subtle) movements of the subject head, we need to compute this movement and correct it.

Since the brain is going to have subtle movements, it can be transformed using 6-parameter affine transformation.

After all the images are processed, all of them are prepared and shares a common coordinate system.

7.1.3 *Unwarping*

Realignment is not the only spatial correction to perform: The scanner does not behaves the same in all brain space. As a Magnetic Resonance Image, it uses a magnetic field to acquire the brain image. This magnetic field, or fieldmap, is distorted by several reasons. So the images are not acquired in a uniform space thus, the image is distorted in some areas. It is possible to correct this space by applying the registered fieldmap.

Unwarping, or also named Fieldmap correction, allows applying this fieldmap mesh into the images from the Time-series, correcting the error produced by magnetic non-uniform fieldmap.

The unwarping option comes with the realignment option, so SPM has two different methods to approach this spatial preprocessing: SPM can perform this realignment method with and without this fieldmap correction option.

For this project, after consider both options (i.e. with and without fieldmap correction), the fieldmap has been considered to retrieve better (less noisy) images.

7.1.4 *Artifact Repair*

Although SPM does a light motion correction in realignment step, it does not correct those images that are too much displaced. Working with HD patients, these kind of movements are very probable because HD patients have problems with motor control: sudden head movements during an experiment are very feasible.

ArtifactRepair [23] is another piece of software used to compute, correct and discard those images with too much movement. This tool computes the interpolation of images between thresholds to correct those images with too much movement registered. These extreme movements can be long or consecutive enough to add noise to several consecutive images. Thus, it is important to control the number of sequential images corrected because we could be interpolating more than two consecutive images.

For this project, the selection of discarded images was set to two consecutive images. This selection is because, with three or more consecutive images, some of the images selected for correction would not have any correct image to interpolate as its neighbour.

7.1.5 *Coregister*

One of the powerful aspects of fMRI is that is fully compatible with structural MRI. Those are images with a much higher definition. By applying another transformation is possible to fit these *"low resolutions"* fMRI into the *"high resolution"* structural MRI.

With another 6-parameter affine transformation it is possible to get both systems (structural MRI and any image from fMRI time-series) into the same coordinate system.

7.1.6 *Segmentation*

This step uses the structural MRI to extract other maps of the brain. With this step, it is possible to attach to a certain subject maps of voxel types: a map of those voxels which are white matter, another one for grey matter and a last one for undesired tissues (bones, eyes, ventricles, etc).

7.1.7 *Normalisation*

Normalisation allows to bring the subject brain into a standard space, so every subject shares the same specific space.

This step is a must when using more than one subject: If a particular voxel (x,y,z) pertains to different structures or tissues for each subject, the results, whichever they are, will not be correct since these voxels can not be compared.

For this step to happen, is very important to fit the coordinate origin of all images to be the same point. When computing this transformation, if this step is not done correctly, the algorithm used can found a local minima and the match between both systems (structural MRI and fMRI) would not fit correctly.

7.1.8 *Smoothing*

In order to reduce the noise, it is used to apply an ending step to smooth the image.

For this project, several smoothing kernel were applied to check the results. Because artifact repair does a little smoothing, depending on if it was used or not this step, a reduced kernel was used to balance this smoothing:

- A smoothing kernel of 8 voxels when not applying artifact repair.
- A smoothing kernel of 7 voxels only if artifact repair step was done.
- A smoothing kernel of 4 voxels when artifact repair step was done.

The final kernel size was 4 voxels because, as observed in the tests done for selecting the smoothing kernel, too much smoothing can affect the resolution of little structures like caudate.

7.2 FIRST LEVEL ANALYSIS

When using SPM to compute fMRI statistics, we expect SPM transform a set of images, to a unique brain map of these active areas for the condition we desire. There are several steps to acquire this brain activity map.

7.2.1 *Specify the Model*

An important point is that, when doing the experiment, the scanner is acquiring all the experiment, with every trial starting at some time and with some duration. The tasks does not fit in a single image, the tasks will start at the middle of some image and finish at the middle of another image. This makes the task for the general linear model more difficult, and to solve that part, the onsets and durations for every desired trial must be specified. With this information SPM has enough information to compute and interpolate all the discrete time-series into their corresponding model.

There are some times that also a condition may be dependant on some variable. Then to extract the information that modulate this variable exist an option in SPM called parametric modulation. For example:

- It may be that for a specific test, the learning rate is high enough that, the most suitable way to extract that learning "interference", is to add the number of each trial as a parametric modulator along with each onset.
- It can be suspected that failing at the trial could affect the brain map because some other function area over-activate. Then adding the result of the trial is the best option.

Finally another option that allows SPM is to declare regressors. Along the same line of parametric modulation, regressors allows the model to skip information of non-desired information by ignoring it at the

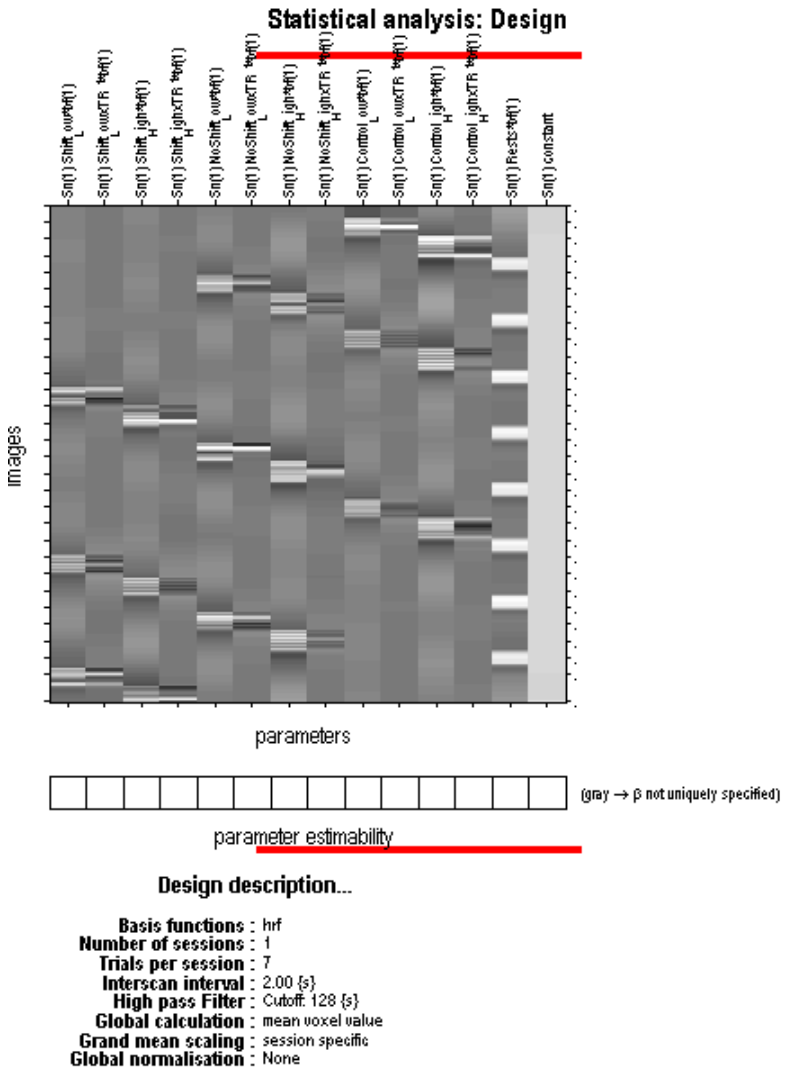

Figure 11: Design Matrix example

level of HRF. A good example of it are the movement estimators extracted from the realingment preprocessing step.

Figure 11 shows a design matrix example. And, for each feature(column) is specified the ”weight” of the corresponding image(row) into that feature.

7.2.2 *Estimation*

Once all this have been specified, we have our Design Matrix, a matrix specifying all the features values for each image. So following the linear regression formulae:

$$Y = X\beta + \epsilon \tag{1}$$

$$Y = X_1\beta_1 + X_2\beta_2 + ... + \epsilon \tag{2}$$

We have on 1 the typical linear regression where, X is the Design matrix we just created that are the features of the model and Y being each one of the images and the targets. So fitting the βs(weights) is just a matter of applying least square method.

Afer this step, all weights for each feature has been estimated into a beta file for each feature/column of the design matrix.

7.2.3 *Factorial Design*

The next step should be the comparison between the weights. The correct way to explain a increased value on the beta file is to compare it with a baseline. If, for example, one feature is the Switch trial and another one is the Identity trial, we can only say that Switch trials activate more the caudate region of the brain if there is a significance difference between the values of Switch and Identity trials. This difference can be computed as a T-statistic or a F-statistic depending on the design of the conditions.

The results of that step produces a contrast image that can be seen later as a brain activity map.

Specifically, in this Thesis, a whole brain analysis was performed for the main contrast of interest (Switch vs. Identity).

7.3 SECOND LEVEL ANALYSIS

All this process where made in order to compute what is named First level analysis. The first level analysis is just to extract the information of just one subject, but this project has 63 subjects splitted in different groups. It can not be said much with just one subject: it may well be an isolated case. These computed files (beta files and contrast files) need to be joined with all the subjects within a group to observe that group's real activations and get rid of individual effects. This step,

named as second level, is made to check if the null hypothesis is given using student's t-test.

For intragroup check, it should be used the one-sample T-test so the results for the test between subjects, being each subject contrast file every data point in the distribution. The result of the one-sample T-test is then a brain map where every voxel is the T value of that one-sample T-test. This result ensures us that these voxels with high T values are going to have more statistical power of being a significative ctived area for that specific contrast. That means that if the Switch - Identity contrast is used for controls group in the one-sample T-test and some area have high T-values, this area is likely to be more actived on Switch trials compared to the Identity baseline.

The two-sample t-test is used also to check if the null hypothesis is given between groups. Being each group contrast images collection each of the t-test distributions, the result is the same: a file where each voxel is the T value. However, the high voxel values correspond to those areas where the first group have more activation than the second in the specified contrast.

8

FMRI RESULTS

Once explained the details and operation of SPM, this part of the Thesis will explain which results we obtained.

As said previously in Section 3, it is interesting to see the region that is known to be activated. And when running the first and second level (Section 7.2) to get the activity brain map just with the original onsets and the result is nothing like as expected, like the table 4, the problem begins.

Region	peak p(FWE)	peak p(FDR)	peak T	x,y,z {mm}		
R Postcentral	0,999	0,999	2,4359	22	-36	46
R Par.Lob.	1	0,999	1,9449	6	-36	58
L Temp.Mid	0,999	0,999	2,378	-38	-52	-2
L Lingual	1	0,999	1,969	-26	-44	-2
R Putamen	0,999	0,999	2,327	26	16	6

Table 4: Activations of Switch - Identity contrast for Controls vs HD on plain onsets

(L) Left, *(R)* Right, *(Par.Lob.)* Parietal Lobule, *(Temp.Mid.)* Temporal Middle Gyrus
All regions are extracted for the values: $clusterp > 0.5$ and $p(unc) < 0.05$

As it can be seen, Table 4 shows very noisy values. Although it can be seen some activation pattern, the p-value selected is so high (p=0.05) that makes the confidence on that activation, summing up the noisy activation map, not that strong.

This could be happening for several reasons. The first to do is compare with previous studies[27] thas shows some significant activity, at least on controls. The study shows that there is an incremental evolution in time of the activation in caudate for shift conditions whereas control conditions have a decremental evolution. This could be perfectly a cause why our caudate is not showing significancy. If the caudate levels are enough similar on both conditions and it is not until later -the last trials of same condition- that we see an superior activa-

tion comparing Switch and Identity. To check this we just needed to check this evolution in time for the caudate. This can be computed as a regressor factor or, in terms of SPM, a parametric modulator. Using the number of each trial as a parametric modulator, all that variance and behaviour explained as a temporal evolution of the trials, will be kept in this feature beta file.

The activated regions seen in table 5 represents the information that those regressors contains. Thus, this high values in caudate region means that, on switch trials, the caudate increment its activity compared to the Identity trials. In fact, if we get the information from Switch and Identity trials and not its regressors, it can not be observed any activation. But this result could be expected: if the incremental activity, and decremental activity of caudate in switch and identity trials, respectively, are substracted (is contained in the number of trials regressors), then the activation could not be significant.

	peak			x,y,z {mm}		
Region	p(FWE)	p(FDR)	T			
L Precentral	6,0E-08	3,4E-06	8,877	-30	-4	58
L Sup.Par.	9,3E-08	3,4-06	8,75	-22	-80	46
R Fusiform	1,2E-05	9,4E-05	7,391	26	-84	-14
L SMA	4,2E-05	0,0002	7,055	-6	8	54
R Precentral	0,002	0,004	6,023	46	0	46
L Thalamus	0,038	0,030	5,144	-26	-28	14
L Caudate	0,187	0,091	4,553	-18	-20	22
R Insula	0,057	0,037	4,487	38	20	6
L Precuneus	0,110	0,062	4,760	-2	-48	6
R Thalamus	0,138	0,0685	4,674	2	-12	6
L Cing.Mid.	0,352	0,172	4,281	-2	-36	26

Table 5: Activations of Switch - Identity contrast for Controls vs HD on Split solution

(L) Left, *(R)* Right, *(Sup.Par.)* Superior Parietal Lobule, *(SMA)* Supplementary Motor Area, *(Cing.Mid.)* Cingulum Middle Gyrus
All regions are extracted for the values: $clusterp < 0.05$ and $p(unc) < 0.001$

Once observed the expected results with this settings of 1st and 2nd level, another set was prepared. If the caudate is really incrementing its activity by time on Switch trials and decrementing it on Identity trials, this activity could be seen on the last part of the block. As a reminder, a block is composer by 12 trials (and there are 3 blocks and an *extra* rest block for each subject), so if the first 6 are splitted from the second 6 trials and only these last 6 are compared, we should be able to get a clear caudate.

However, there are some activations that lead to think that there is something more involved. Reading some more on [27] shows that

another of the differences is that all the wrong trials have been discarded. This is an important issue in neuroscience, since wrong responses may activate a different newtork, we must process the design matrix, extracting those wrong responses from the design matrix.

To corroborate both, correct answers and incremental activity on caudate, it was decided to take some time computing several design matrices. In those, the trials were not splitted into two different regressors, but only the correct higher trials were kept, keeping for each condition, the same number of trials from the last part of the block. Finally, several solution with similar (18,20,21,23) trials was kept. These solutions showed that the more trials kept, the less signal on caudate was found.

But, after some discussion and other design matrices, it was agreed that those were different designs. The fact that the first part of the images were not kept in the experiment in a design matrix (in any linear model) make the model different, as the model part of these first trials could not be explained with the other features. Hence, the algorithm can not fit a proper model. So finally, a desgin matrix with only correct trials[27] but with splitting the low and high part was decided to kept.

Region	peak p(FWE)	peak p(FDR)	T	x,y,z {mm}		
L Precentral	2,6E-07	1,3E-05	9,020	-50	0	38
L Sup.Par.	3,6E-06	4,9E-05	8,175	-22	-80	46
L SMA	0,0001	0,0008	6,970	-6	4	58
R SMA	0,230	0,136	4,602	10	4	58
R Sup.Occ.	0,0002	0,0008	6,898	26	-64	38
R Lingual	0,0003	0,0009	6,781	26	-88	-14
R Precetral	0,010	0,011	5,743	46	0	46
R Sup.Front.	0,0612	0,045	5,145	6	24	62
L Thalamus	0,076	0,050	5,061	-26	-28	14
L Caudate	0,372	0,177	4,373	-18	-20	22
R Insula	0,311	0,157	4,462	34	16	6

Table 6: Activations of Switch - Identity contrast for Controls vs HD on Split solution with only correct trials

(L) Left, *(R)* Right. *(Sup.Par.)* Superior Parietal Lobule, *(SMA)* Supplementary Motor Area, *(Sup.Occ.)* Superior Occipital Gyrus, *(Sup.Front.)* Superior Frontal Gyrus
All regions are extracted for the values: $clusterp < 0.05$ and $p(unc) < 0.001$

Finally, it was concluded to better add the reaction time of response to the model. Since the fact that large reaction times can be producing some undesired activation, by adding a regressor that take into account this effect could be of use.

In Figure 12 the activation brain map for Controls can be seen.

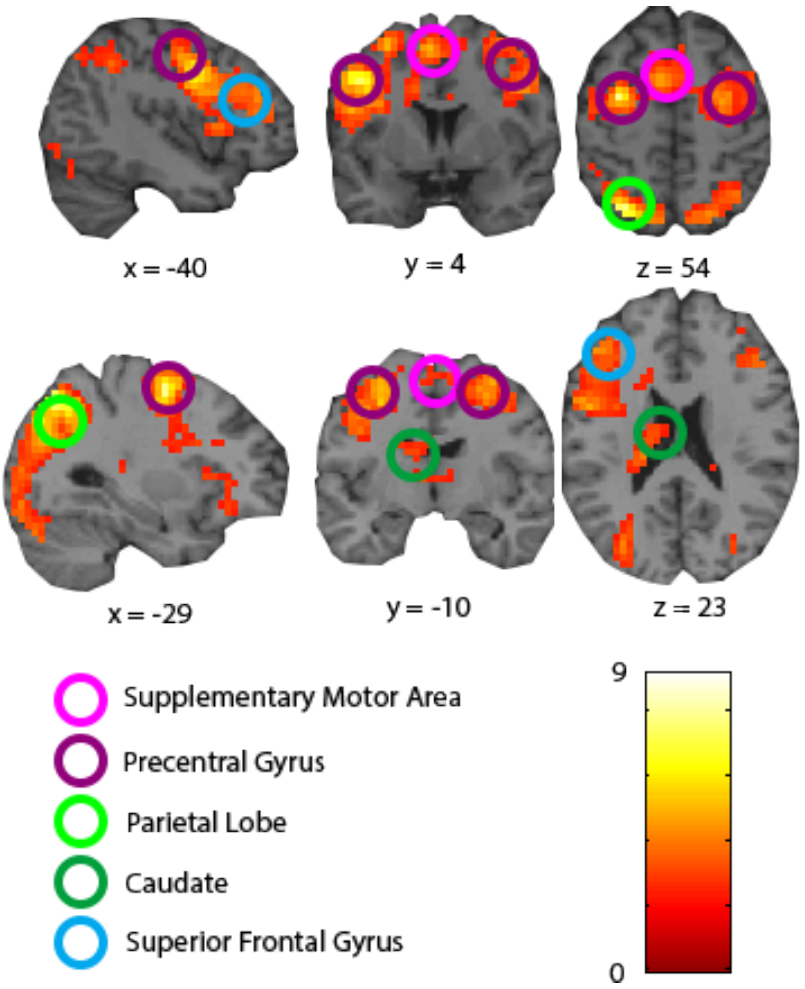

Figure 12: Activity map of Switch - Identity contrast for Controls group on Split solution with only correct trials and Reaction Time as regressor

When comparing between control and HD group, can be seen that, those same regions, are significantly more activated by Controls (see Figure 13).

Consistent with typical findings form the task-switching literature [27][18][3], both Controls and Patient engaged in the switching process the dorsolateral frontoparietal circuit, including subcortical activations in the in the left caudate and in the left thalamus (e.g. see Figure 12 for Controls activity activation).

As it has showed in Figure 13 and Table 7), a two-sample t-test between Controls and HD patients revelaed significant lower levels of activity in the frontoparietal network and the caudate nucleus in HD patients.

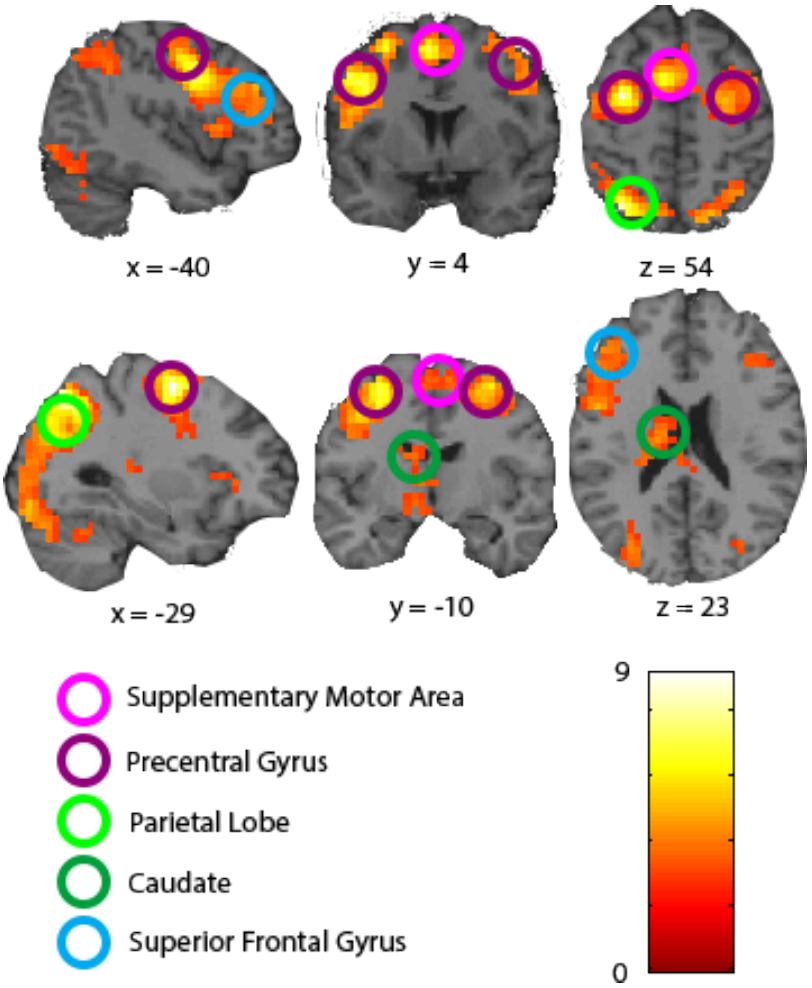

Figure 13: Activity map of Switch - Identity contrast for Controls vs HD on Split solution with only correct trials and Reaction Time as regressor

Interestingly, another two-sample t-test between Controls and PreHD subects also revealed significant difference between both groups activation in the frontoparietal network and the caudate nucleus (See Figure 14 and Table 8).

Region	peak p(FWE)	p(FDR)	T	x,y,z {mm}		
L Precentral	2,0E-07	5,6E-06	9,119	-30	-4	58
L Parietal Sup	2,1E-07	5,6E-06	9,096	-22	-80	46
L SMA	0,0001	0,0005	7,0125	-6	4	58
R SMA	0,309	0,141	4,478	10	0	58
R Occipital Sup	0,0004	0,001	6,701	26	-64	38
R Parietal Sup	0,084	0,051	5,033	22	-76	50
R FusiForm	0,0005	0,001	6,645	26	-84	-14
R Frontal Mid	0,004	0,005	6,017	34	-8	62
R Precentral	0,074	0,051	5,083	50	0	46
L Thalamus	0,0915	0,051	5,001	-26	-28	14
L Caudate	0,496	0,215	4,228	-14	-16	22

Table 7: Activations of Switch - Identity contrast for Controls vs HD on Split solution with only correct trials and Reaction Time as regressor

All regions are extracted for the values: $clusterp < 0.005$ and $p(unc) < 0.001$

Region	peak p(FWE)	p(FDR)	T	x,y,z {mm}		
L Parietal Sup	5,0E-07	4,3E-05	9,545	-22	-80	46
L Occipital Mid	1,3E-06	5,1E-05	9,165	-26	-80	38
L Parietal Inf	8,6E-06	0,0001	8,465	-30	-68	46
L Precetral	4,2E-06	9,2E-05	8,733	-30	-4	54
L Precentral	1,0E-05	0,0001	8,409	-46	-4	34
L Precentral	0,0008	0,004	6,831	-38	-4	42
R Occipital Inf.	5,3E-05	0,0004	7,807	34	-84	-10
R Occipital Inf.	0,003	0,009	6,349	30	-88	-2
Cerebellum	0,171	0,074	5,018	14	-80	-26
R Occipital Sup	0,002	0,007	6,539	26	-68	38
R Occipital Mid	0,0290	0,0276	5,620	34	-76	38
R Parietal Sup	0,097	0,049	5,211	22	-72	54
R Frontal Sup.	0,011	0,018	5,937	34	-4	62
R precentral	0,032	0,028	5,583	50	8	34
L SMA	0,048	0,033	5,449	-6	4	58
L Thalamus	0,022	0,025	5,717	-26	-32	18
L Caudate	0,343	0,137	4,679	-22	-28	22

Table 8: Activations of Switch - Identity contrast for Controls vs PreHD on Split solution with only correct trials and Reaction Time as regressor

All regions are extracted for the values: $clusterp < 0.005$ and $p(unc) < 0.001$

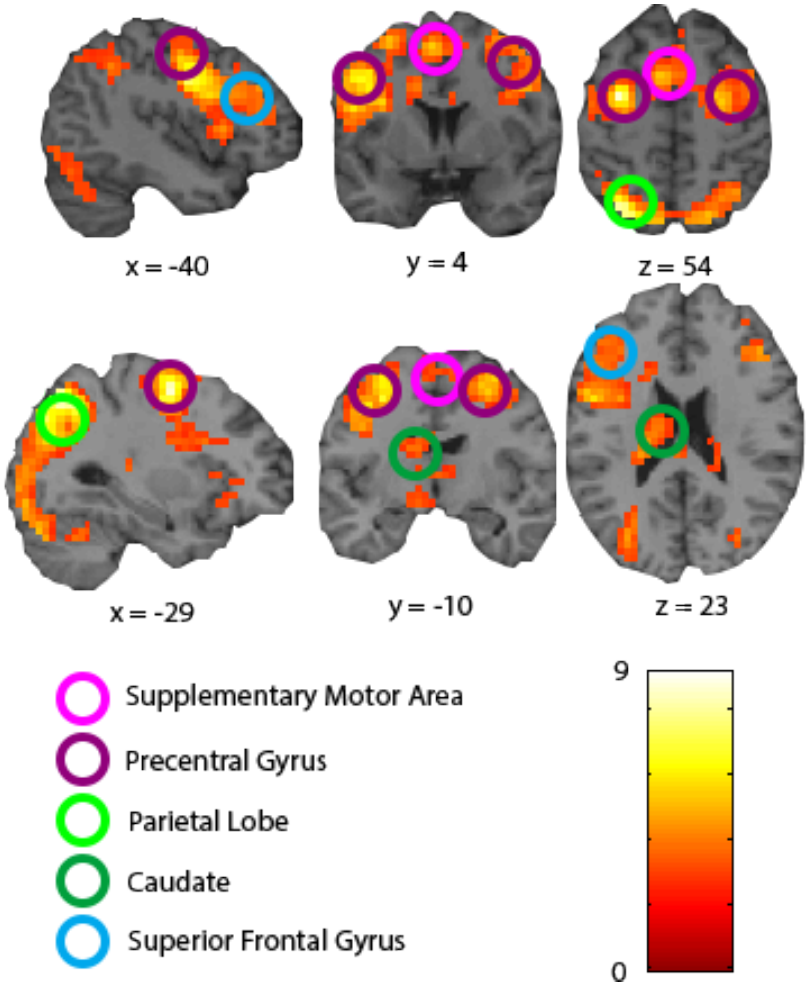

Figure 14: Activity map of Switch - Identity contrast for Controls vs PreHD on Split solution with only correct trials and Reaction Time as regressor

Part III

MACHINE LEARNING APPROACH

9

MACHINE LEARNING

Since subtle changes in brain may not produce a statistical significance between voxels, general linear model may not able to detect very early stages of HD. Although it can detect regions affected in advanced HD patients, is difficult to detect the initial changes of PreHD patients. However, machine learning techniques use a multi-variate approach to detect a massive collection of subtle changes significant enough to explain a cognitive presymptomatolgy.

Therefore, the use of machine learning techniques to find biomarkers that can explain this congitive presymptomatology can help determining the status of a PreHD patient.

In order to determine this, a classification will be proceeded with two different approaches:

PRONTO A Pattern Recognition software using machine learning techniques.

SVM WITH FLDA Solution proposed as a comparison for Pronto software.

9.1 PRONTO

When launching Pronto software a GUI is showed with several options. In a "**Main steps**" box there are the options to construct an run our classificator at the left:

- Data & Design
- Prepare feature set
- Specify model
- Run model
- Compute Weights

And the "**Review options**" box at right serve to check the results:

- Review data
- Review Kernel & CV
- Display results

Finally there is an option "**Batch**" to open the matlabbatch editor, so batch scripts can be coded for any step. Although the first step "Data & Design" could be scripted with matlabbatch, the next step "Prepare feature set" could not be run yet.

9.1.1 *Data & Design*

The first that must be done in every kind of analysis is to prepare the dataset. On this step, the user should fill every subject and every modality it has. This step is not to create the dataset, but to declare all data that can be used in different datasets. Filling with all data will allow future reutilisation of the same structure. Even if the user has a modality (EEG ie) and he is not going to use it in the next classifications, but does not discard using them in the near future, the best option is to include it. To do it, simply add a Group and, for any subject you add, modalities have to be manually introduced along with its files.

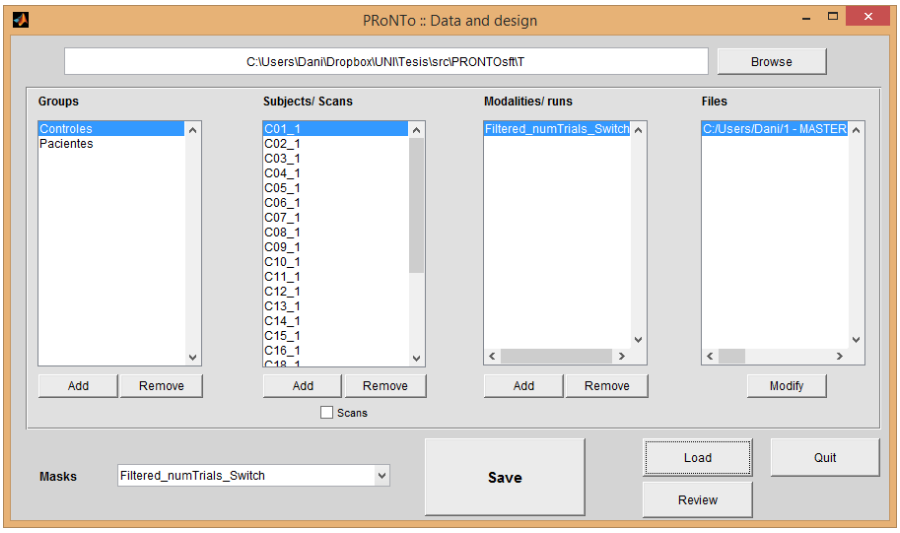

Figure 15: Data & Design window

When including the data, an *SPM.mat* must be specified in order to set the desired onsets, if it is not available, manual entry of onsests are requested. After including all data, one must be sure to introduce mask for every modality and the output folder of *PRT.mat*.

PRT.mat is a file that keeps all the information of a specific dataset in pronto. A PRT.mat can point to several feature sets and models.

Although the information on feature sets are on a different file, PRT file points to it so that is the reason why one should include all data possible into the first run.

9.1.2 *Prepare feature set*

In the previous section it was defined all the data of the experiment. In this step the dataset is going to be defined. Whether if the experiment will focus on all the brain data or a specific region of the brain, use only one modality or various, all that is going to set in the window from figure 16.

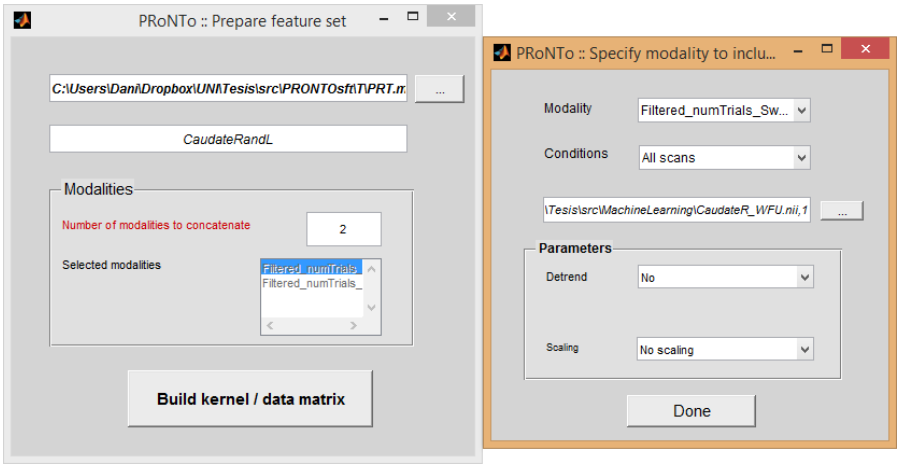

Figure 16: Prepare feature set window

9.1.3 *Specify model*

After the dataset is defined. The last step is just define the model with figure 17 window. As always, selecting *PRT.mat* will enable the "**Feature set**" and after naming the model and selecting one of the specified feature sets, the classification/regression model must be specified.

This step also allows the user to apply some preprocessing to the data before running the model.

9.1.4 *Run model*

This section allows the user to re-run a specified model. Because there exist the option to specify and run the model in the specify model step, this option is not that useful.

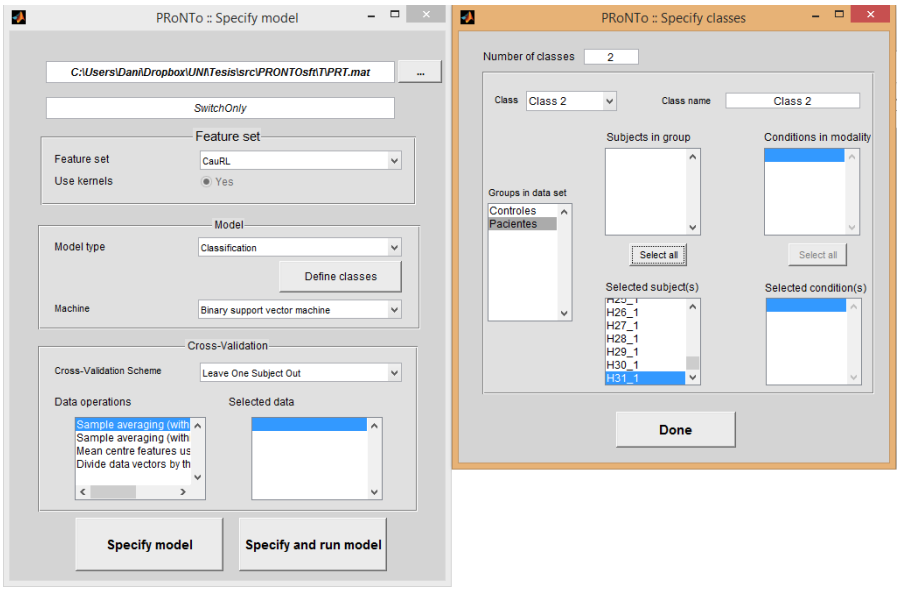

Figure 17: Specify model window

9.1.5 *Compute Weights*

Once the model has been computed, the direct results are the predictions and the performance of the model. However, in Neuroscience field, understanding why this model is predicting that, the retrieval of weights in a brain map-like format is as desired as the performance itself.

With this option, the user can select the computed model of a PRT file and collect the weights in the shape of a brain map.

9.1.6 *Review data*

Review data section is useful to check the onsets and conditions of the model. It shows to the user the number of each conditions in a simple bar plot.

9.1.7 *Review Kernel & CV*

How to know before computing weights that our model has been modelled correctly? This section allows a quick review of the model - to check everything was set where it should(controls on control group and patients in patient group)-, the Cross Validation configuration or even the Kernel computed. This is a great feature since, seeing a "constant" kernel will reveal that something went wrong.

9.1.8 *Display results*

The last option allows to show the results of the performance of the model. In the top part, usual performance values can be accessed:

HISTOGRAM Plot of sample distributions by classes.

CONFUSION MATRIX The confusion matrix allows to a quick visual check on the performance and also allows to compute othe derived performance values

PREDICTIONS Useful if there are any outlier.

ROC CURVE Usual measure for classificators.

On the lower part, two different spaces for loading brain maps are found. The left one is for the computed weight image. Sadly, the visualization of that image is very poor so the box on the right can be used to load a brain reference image. A canonical T1 image is perfect for navigating the brain and observe, at the left, the weight it has on the computed model.

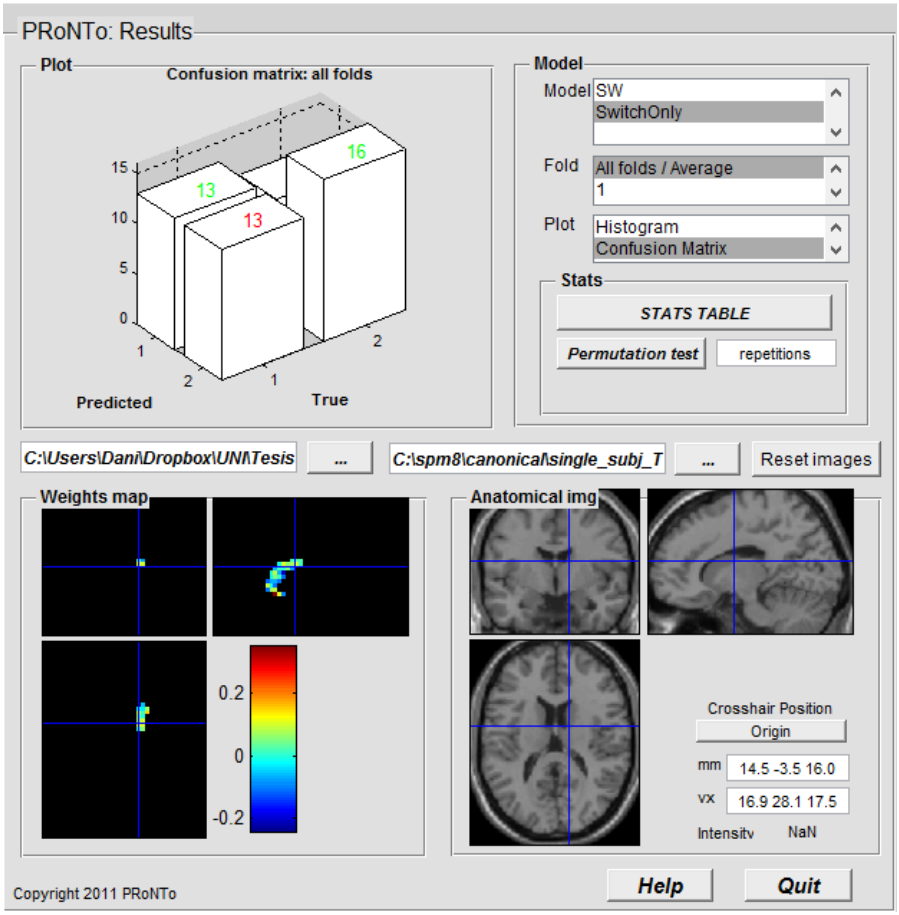

Figure 18: Display results window

9.2 SVM WITH FLDA

Because of several errors, manual settings and some restictions, the student thought about implementing a quick Machine Learning algorithm based on SVM[24][29][31].

For the data, it was desired to use the same files that SPM compute as beta files and contrast files. SPM compute the HRF basis function, the onsets and use a General Linear Model to compute that beta and contrast files. Using these files instead of directly fMRI can save us much more efforts on feature reduction. If the fMRI were to be used, the feature set will increment to: $40 * 48 * 34$(voxels in one 3D image)$*477$(images in a time series) $>= 31$ Millions of features per subject. Also, the number of images can vary from subject to subject because there are subjects (patients almost) that have less images due to different problems. By selecting the features directly from the beta files and/or contrast files, the feature number is reduced drastically. But there are still so many features for the SVM to handle properly.

9.2.1 *Extracting the features*

But the betas and contrasts files are still too large. For that reason, the best feature for the proble will be one feature describing each interesting area of each file. For example, if the desired areas are Caudate and Prefrontal cortex, a combination of the voxels of those area for each file would be the best solution. In fact, knowing the area, can be easily extrapolate to mask those areas and, for its peak, extract an spherical ROI to compute that feature extraction. Since the activation burst is what is expected to be the most informative as a predictor, the fact that the feature extraction is centered at the activation peak should help the feature extractor.

For the later part, some works, even with HD topic, have also used LDA[28] as a feature extraction method for a SVM. Since it is a supervised problem what this thesis is facing, the discrimination of features by using the information about the different classes should extract better components.

9.2.2 *Fisher Linear Discriminant Analysis*

The code used for the LDA part has been extracted from[5]. This package allows to extract the components using Fisher LDA with a simple call as:

Source 9.1: Use of LDA

```
options = [];
options.Fisherface = 1;
[eigVectors,eigValues] = LDA(y,options,X);
```

9.2.3 *Support Vector Machine*

In order to test a first solution and observe its performance, a RBF SVM was choosen for its capability of to have a better performance in classification. At least the same performance as a linear SVM

Hence, SVM in its dual form is used. Since we are using CVXr[8], we need to code the convex language of the SVM in its dual form:

$$\begin{aligned} \underset{v}{\text{maximize}} \quad & v^T 1 - \frac{1}{2} v^T Q v \\ \text{subject to} \quad & 0 >= v_i >= \lambda, \forall i = 1, \ldots, N \\ & v^T y = 0 \\ \text{where} \quad & Q = diag(y) K diag(y) \end{aligned} \tag{3}$$

Into Matlab code using cvx convex language:

Source 9.2: SVM dual form

```
Q = diag(labels)*Kernel*diag(labels);

cvx_begin quiet
    variables v(m);
     maximize( v'*ones(size(v)) - 0.5*v'*Q*v )
    subject to
    0 <= v;
    v <= lambda;
    v'*labels == 0;
cvx_end
```

For selecting sigma and lambda values, a grid search has been implemented with a nested cross-validation. The inner folds were used to train SVM with the grid values(sigma and lambda) and then, the validation of the models was done in the outer folds.

From the grid search of values:

- sigma = [0.0001 0.001 0.1 0.5 1 5 10]
- lambda =[0 1 5 10 25 50 100]

10

MACHINE LEARNING RESULTS

In order to compare the efficiency of the different approaches used, different statistical measures based on classification confusion matrix are going to be applied. In particular the confusion matrix, and the measures extracted from it (i.e. accuracy, precision, recall, specificity and F1-score):

Confusion Matrix is used to explain the performance of the classifier. All the predictions of the classifier are counted and organized in a table by type as it can be seen in Table 9.

		True	
		Positive	Negative
Pedicted	Positive Patients	True Positive	False Positive
		False Negative	True Negative

Table 9: Confusion Matrix

$$\text{accuracy} = \frac{\text{True Positive + False Positive}}{\text{True Positive + True Negative + False Positive + False Negative}} \tag{4}$$

Accuracy is the measure to observe the percentage of samples well classified.

$$\text{precision} = \frac{\text{True Positive}}{\text{True Positive + False Positive}} \tag{5}$$

Precision measure the proportion of real positives predicted among all samples predicted as positive.

$$\text{recall} = \frac{\text{True Positive}}{\text{True Positive + False Negative}} \tag{6}$$

Recall measures the percentage of positives which are correctly identified.

$$\text{specificity} = \frac{\text{True Negative}}{\text{True Negative + False Positive}} \tag{7}$$

Specificity is the measure that computes the number of negative that has been really negative.

$$\text{F1-score} = 2\frac{\text{Precision} \cdot \text{Recall}}{\text{Precision+Recall}} \tag{8}$$

A combined measure that takes into account Precision and Recall measues. It can be interpreted as a weighted accuracy, since the balance between precision and recall gives the measure higher values.

10.1 FIRST TEST

Since we expect that caudate is one of the main regions our first approach was to mask our switch condition contrast (switch vs Identity) with the caudate that had been segmented previously form the structural T1 image.

The first model that we apply try to classify HD patients and Controls but the classification fails.

		True	
		Controls	Patients
Pedicted	Controls	13	13
	Patients	11	16

Table 10: First test confusion matrix

Statistical measures can be extracted from the confusion matrix (Table 10).

10.2 SECOND TEST

Therefore, in order to increase the accuracy to the classifier we add more information to it. In particular:

FMRI The whole fMRI data is being used on this test.

SPM.MAT As fMRI data is being used, to specify onsets, the split solution with only correct trials and reaction time as regressor was used.

MASKS Using mask of results areas in feature set definition.

Accuracy	Precision	Recall	Specificity	F1 score
0,547	0,542	0,5	0,593	0,542

Table 11: First test performance

As for the masks, those significant areas in Conventional Analysis were used:

- Caudate L
- Caudate R
- Parietal Superior L
- Parietal Superior R
- Precentral L
- Precentral R
- Supplementary Motor Area L
- Supplementary Motor Area R

After setting these masks, the model was run for another Control / Patients model obtaining results shown in table 12.

		True	
		Controls	Patients
Pedicted	Controls	14	12
	Patients	14	12

Table 12: Second test confusion matrix

However, despite the introduction of all fMRI data and the masks for each region of interest, this approach still does not work. As it can be seen in the results (See table 13).

10.3 THIRD TEST

The previous tests were using Patients and Controls as classes. But, being PreHD patients among HD patients, could make much noise to the classifier. For the next test, the same data as the second test is used. The difference relies in the model specification, where this time is set to use controls and only symptomatic HD patients. With that configuration the classifier have a better classification as it can be seen in its confusion matrix (See table 14).

And the different statistical measures (See table 15).

Accuracy	Precision	Recall	Specificity	F1 score
0,5	0,5	0,538	0,462	0,497

Table 13: Second test performance

		True	
		Controls	Patients
Pedicted	Controls	19	7
	Patients	14	12

Table 14: Third test confusion matrix

Accuracy	Precision	Recall	Specificity	F1 score
0,682	0,731	0,731	0,611	0,666

Table 15: Third test performance

10.4 SVM USING FLDA

On the other hand, the classifier developed in Idibell could not use fMRI properly. So for this solution, the dataset was based on the Switch vs Identity Contrast file of the conventional analysis last result Also, the same list mask as in section 10.2 to extract features was used.

For the SVM parameter selection, from the grid (Section 9.2), the best obtained values are:

- sigma = 0.1
- lambda = 1

The results are shown in the confusion matrix for the 3 outer folds (Table 16):

		True	
		Controls	Patients
Pedicted	Controls	17	10
	Patients	9	8

Table 16: SVM + FLDA confusion matrix

From that confusion matrix, it can be extracted the statistical measures:

Accuracy	Precision	Recall	Specificity	F1 score
0,568	0,63	0,654	0,444	0,529

Table 17: SVM + FLDA solution performance

10.5 DISCUSSION ON MACHINE LEARNING RESULTS

Using all the results in a table (Table 18) to compare, we obtain:

	Accuracy	Precision	Recall	Specificity	F1 score
First test	0,547	0,542	0,5	0,593	0,542
Second test	0,5	0,5	0,538	0,462	0,497
Third test	0,682	0,731	0,731	0,611	0,666
SVM + LDA	0,568	0,63	0,654	0,444	0,529

Table 18: Performance values of the different machine learning tests

For controls and HD patients classification, the third test is better in all parameters. However, each test is not truly comparable with each other since they have different dataset inputs (i.e. first test had Switch vs Identity contrasts with caudate mask, second and third test includes all fMRI with several masks and the SVM with FLDA solution used Swich vs Identity contrasts and several masks) and different models (i.e. first and second test models Control class against HD and PreHD class, meanwhile third and SVM with FLDA solution models Control class against only HD class). But, taking into account the low accuracies achieved by first and second tests, the explanation is that, with these models and the information we have, we cannot predict between Controls and Patients (being of PreHD or HD group). This may well be because the introduction of PreHD in a class that may be closer to Control group than HD group in terms of brain activity.

Contrary to first and second level, the third test has an acceptable, yet improvable, accuracy. Furthermore, not only has better % of well classified samples, but also that the false positives and false negatives are better are balanced as it can be seen with precision and recall measures. In general, with a F1 score of 66% is the best classifier despite being a quite low compared to other machine learning applications. It can be said that, with these values, it is possible to classify Controls and HD groups, contrary to Controls and Patients model.

Part IV

RESULTS

11

CONCLUSIONS

A whole brain analysis was performed for the main contrast of interest (Switch vs. Identity). For the fMRI analysis, both the first trial of each condition and errors were removed. As it was reported by Monchis et al. [27], we observed that the the caudate nucleus in the Switch condition showed a significant correlation between the level of BOLD signal and the increased trial position (as the time since the last set shift increases) while it decreased over time in the Identity Condition. Therefore, in order to optimise the difference between both conditions (Switch and Identity), we split the block length for each condition and we only reported the effects observed in the last half part of the block. Moreover, since Patients and Controls showed significant main effects and interactions in reaction times (RT) between conditions, RT times were regressed in the analysis. All activations we report were corrected for multiple comparison (FDR) at cluster level p¡ 0.05.

Consistent with typical findings form the task-switching literature [18][27][3], both Controls and Patient engaged in the switching process the dorsolateral frontoparietal circuit, including subcortical activations in the in the left caudate and in the left thalamus (see Figure 13 and Table 7).

As it has showed in Figure 13 and Table 7), a two-sample t-test between Controls and HD patients revelaed significant lower levels of activity in the frontoparietal network and the caudate nucleus in HD patients. Importantly, pre-HD patients also show a reduced significant activity in the dorsolateral prefrontal cortex and the striatum before symptoms begin.

Also the classification allow us to classify between control and HD group with an acceptable, yet improvable, accuracy. These results, accordingly with fMRI analysis shows that it is possible to classify between groups with only some masks of some desired regions. However, the low accuracy of classification between Controls and Patients (PreHD and HD group), make impossible the classification.

11.1 FUTURE WORK

Individual differences study in HD is of utmost importance in clinical essays. It will allow to classify HD patients into different profiles to get more homogeneous groups of patients, which is important when evaluating a new drug efficiency and, in HD case, essential given the high variability of the prevalence on different symptoms on this disease. It will also be possible to predict the symptomathology type developed by each patient, being that a new possibility to preventive treatment.

The work done in this Thesis opens much work to be done and some new questions on this field.

Of the proposed solution (Chapter 9), only the classification of HD and Control group has been done. There is still work to do and to improve on both approaches of the solution and the Idibell HD projecthas not finished yet.

Using the first approach, temporal information of fMRI scans have been used in Pronto toolbox, selecting only the desired areas to be used on a binary classification using Support Vector Machines (SVM). So there are some improvements to be done:

MULTIMODALITY Only fMRI has been tried on classification. Although regression does not allow multi-modality, classification does it. The inclusion of external data to infer some information of the fMRI scans may be of great importance: Age, brain atrophy, disease burden can be of great impact on some studies as it could give to the SVM more variability explanation.

OTHER METHODS Pronto can use several machine learning methods for classification. Among the 3 available methods (i.e. SVM, binary Gaussian Processes classification and multi-class Gaussian Processes classification) only the first one was.

Said that, Pronto works with the data, preprocessed or not, of several modalities for classifiers and only one modality/value for regression. The toolbox is also very restrictive of what to declare as an input and there are several applications for what is not prepared like, for example, adding external features like it could be age, VBM or alike.

With the second approach Fisher Linear Discriminant Analysis(FLDA) is used as a feature extractor to characterise the different interesting areas extracted from fMRI analysis files(Chapter 8), with a single linear component of the area voxels for the classifier. A binary SVM is the used on

On the other hand, the second classifier has much more room to improve:

MULTIMODALITY Only one image was used as input of the classifier to test both classifiers, although it can easily be expanded to more images or other values.

FEATURE EXTRACTION This solution can be highly improved by selecting better features.

FMRI DATA Pronto can work easily with fMRI scans: All the information is in the fMRI scans. The inclusion of fMRI data could give more information and variability although it would mean to improve, even more, the feature extraction part. However, taking into account the difficulty to extract good SPM contrast files, this could be a good improvement.

Once the solutions are ready and can be repeated for all the classifications (Section 9.2), the ECOC architecture can be implemented.

BIBLIOGRAPHY

[1] J. S. Anderson, J. A. Nielsen, A. L. Froehlich, M. B. DuBray, T. J. Druzgal, A. N. Cariello, J. R. Cooperrider, B. A. Zielinski, C. Ravichandran, P. T. Fletcher, A. L. Alexander, E. D. Bigler, N. Lange, and J. E. Lainhart. Functional connectivity magnetic resonance imaging classification of autism. *Brain*, 134(12):3742–3754, oct 2011.

[2] F. DuBois Bowman. Brain imaging analysis. *Annual Review of Statistics and Its Application*, 1(1):61–85, 2014.

[3] Todd S Braver, Jeremy R Reynolds, and David I Donaldson. Neural mechanisms of transient and sustained cognitive control during task switching. *Neuron*, 39(4):713–726, 2003.

[4] Matthew Brett, Jean-Luc Anton, Romain Valabregue, and Jean-Baptiste Poline. Region of interest analysis using an spm toolbox. *NeuroImage*, 16(2), Jun 2002.

[5] Deng Cai, Xiaofei He, and Jiawei Han. Training linear discriminant analysis in linear time. In *Proc. 2008 Int. Conf. on Data Engineering (ICDE'08)*, 2008.

[6] Alex Fornito, Andrew Zalesky, and Michael Breakspear. The connectomics of brain disorders. *Nature Reviews Neuroscience*, 16(3):159–172, feb 2015.

[7] Michael Grant and Stephen Boyd. Graph implementations for nonsmooth convex programs. In V. Blondel, S. Boyd, and H. Kimura, editors, *Recent Advances in Learning and Control*, Lecture Notes in Control and Information Sciences, pages 95–110. Springer-Verlag Limited, 2008. `http://stanford.edu/~boyd/graph_dcp.html`.

[8] Michael Grant and Stephen Boyd. CVX: Matlab software for disciplined convex programming, version 2.1. `http://cvxr.com/cvx`, March 2014.

[9] M.A. Gray, G.F. Egan, A. Ando, A. Churchyard, P. Chua, J.C. Stout, and N. Georgiou-Karistianis. Prefrontal activity in huntington's disease reflects cognitive and neuropsychiatric disturbances: The IMAGE-HD study. *Experimental Neurology*, 239:218–228, jan 2013.

[10] Deborah L. Harrington, Dawei Liu, Megan M. Smith, James A. Mills, Jeffrey D. Long, Elizabeth H. Aylward, and Jane S. Paulsen.

Neuroanatomical correlates of cognitive functioning in prodromal huntington disease. *Brain and Behavior*, 4(1):29–40, 2014.

[11] IBM Corp. IBM SPSS Statistics for Windows, Version 19.0. *Armonk, NY: IBM Corp*, 2010.

[12] Sandra Close Kirkwood, Eric Siemers, Julie C. Stout, M. E. Hodes, P. Michael Conneally, Joe C. Christian, and Tatiana Foroud. Longitudinal cognitive and motor changes among presymptomatic huntington disease gene carriers. *Archives of Neurology*, 56(5):563, may 1999.

[13] S. Kloppel, C. Chu, G. C. Tan, B. Draganski, H. Johnson, J. S. Paulsen, W. Kienzle, S. J. Tabrizi, J. Ashburner, and R.S.J. Frackowiak. Automatic detection of preclinical neurodegeneration: Presymptomatic huntington disease. *Neurology*, 72(5):426–431, feb 2009.

[14] S. Kloppel, C. M. Stonnington, J. Barnes, F. Chen, C. Chu, C. D. Good, I. Mader, L. A. Mitchell, A. C. Patel, C. C. Roberts, N. C. Fox, C. R. Jack, J. Ashburner, and R. S. J. Frackowiak. Accuracy of dementia diagnosis–a direct comparison between radiologists and a computerized method. *Brain*, 131(11):2969–2974, jun 2008.

[15] S. Li, F. Shi, F. Pu, X. Li, T. Jiang, S. Xie, and Y. Wang. Hippocampal shape analysis of alzheimer disease based on machine learning methods. *American Journal of Neuroradiology*, 28(7):1339–1345, aug 2007.

[16] Joseph A Maldjian, Paul J Laurienti, Robert A Kraft, and Jonathan H Burdette. An automated method for neuroanatomic and cytoarchitectonic atlas-based interrogation of fMRI data sets. *Neuroimage*, 19(3):1233–1239, Jul 2003.

[17] O. Monchi, J.G. Taylor, and A. Dagher. A neural model of working memory processes in normal subjects, parkinson's disease and schizophrenia for fmri design and predictions. *Neural Networks*, 13(89):953 – 973, 2000.

[18] Oury Monchi, Michael Petrides, Antonio P. Strafella, Keith J. Worsley, and Julien Doyon. Functional role of the basal ganglia in the planning and execution of actions. *Annals of Neurology*, 59(2):257–264, 2006.

[19] M. Mur, P. A. Bandettini, and N. Kriegeskorte. Revealing representational content with pattern-information fMRI–an introductory guide. *Social Cognitive and Affective Neuroscience*, 4(1):101–109, nov 2008.

[20] B. Mwangi, K. P. Ebmeier, K. Matthews, and J. Douglas Steele. Multi-centre diagnostic classification of individual structural

neuroimaging scans from patients with major depressive disorder. *Brain*, 135(5):1508–1521, apr 2012.

[21] Adam C. Naj, Gyungah Jun, Christiane Reitz, Brian W. Kunkle, William Perry, Yo Son Park, Gary W. Beecham, Ruchita A. Rajbhandary, Kara L. Hamilton-Nelson, Li-San Wang, John S. K. Kauwe, Matthew J. Huentelman, Amanda J. Myers, Thomas D. Bird, Bradley F. Boeve, Clinton T. Baldwin, Gail P. Jarvik, Paul K. Crane, Ekaterina Rogaeva, M. Michael Barmada, F. Yesim Demirci, Carlos Cruchaga, Patricia L. Kramer, Nilufer Ertekin-Taner, John Hardy, Neill R. Graff-Radford, Robert C. Green, Eric B. Larson, Peter H. St. George-Hyslop, Joseph D. Buxbaum, Denis A. Evans, Julie A. Schneider, Kathryn L. Lunetta, M. Ilyas Kamboh, Andrew J. Saykin, Eric M. Reiman, Philip L. De Jager, David A. Bennett, John C. Morris, Thomas J. Montine, Alison M. Goate, Deborah Blacker, Debby W. Tsuang, Hakon Hakonarson, Walter A. Kukull, Tatiana M. Foroud, Eden R. Martin, Jonathan L. Haines, Richard P. Mayeux, Lindsay A. Farrer, Gerard D. Schellenberg, Margaret A. Pericak-Vance, Marilyn S. Albert, Roger L. Albin, Liana G. Apostolova, Steven E. Arnold, Robert Barber, Lisa L. Barnes, Thomas G. Beach, James T. Becker, Duane Beekly, Eileen H. Bigio, James D. Bowen, Adam Boxer, James R. Burke, Nigel J. Cairns, Laura B. Cantwell, Chuanhai Cao, Chris S. Carlson, Regina M. Carney, Minerva M. Carrasquillo, Steven L. Carroll, Helena C. Chui, David G. Clark, Jason Corneveaux, David H. Cribbs, Elizabeth A. Crocco, Charles DeCarli, Steven T. DeKosky, Malcolm Dick, Dennis W. Dickson, Ranjan Duara, Kelley M. Faber, Kenneth B. Fallon, Martin R. Farlow, Steven Ferris, Matthew P. Frosch, Douglas R. Galasko, Mary Ganguli, Marla Gearing, Daniel H. Geschwind, Bernardino Ghetti, John R. Gilbert, Jonathan D. Glass, John H. Growdon, Ronald L. Hamilton, Lindy E. Harrell, Elizabeth Head, Lawrence S. Honig, Christine M. Hulette, Bradley T. Hyman, Gregory A. Jicha, Lee-Way Jin, Anna Karydas, Jeffrey A. Kaye, Ronald Kim, Edward H. Koo, Neil W. Kowall, Joel H. Kramer, Frank M. LaFerla, James J. Lah, James B. Leverenz, Allan I. Levey, Ge Li, Andrew P. Lieberman, Chiao-Feng Lin, Oscar L. Lopez, Constantine G. Lyketsos, Wendy J. Mack, Frank Martiniuk, Deborah C. Mash, Eliezer Masliah, Wayne C. McCormick, Susan M. McCurry, Andrew N. McDavid, Ann C. McKee, Marsel Mesulam, Bruce L. Miller, Carol A. Miller, Joshua W. Miller, Jill R. Murrell, John M. Olichney, Vernon S. Pankratz, Joseph E. Parisi, Henry L. Paulson, Elaine Peskind, Ronald C. Petersen, Aimee Pierce, Wayne W. Poon, Huntington Potter, Joseph F. Quinn, Ashok Raj, Murray Raskind, Barry Reisberg, John M. Ringman, Erik D. Roberson, Howard J. Rosen, Roger N. Rosenberg, Mary Sano, Lon S. Schneider, William W. Seeley, Amanda G. Smith, Joshua A. Son-

nen, Salvatore Spina, Robert A. Stern, Rudolph E. Tanzi, Tricia A. Thornton-Wells, John Q. Trojanowski, Juan C. Troncoso, Otto Valladares, Vivianna M. Van Deerlin, Linda J. Van Eldik, Badri N. Vardarajan, Harry V. Vinters, Jean Paul Vonsattel, Sandra Weintraub, Kathleen A. Welsh-Bohmer, Jennifer Williamson, Sarah Wishnek, Randall L. Woltjer, Clinton B. Wright, Steven G. Younkin, Chang-En Yu, and Lei Yu. Effects of multiple genetic loci on age at onset in lateonset alzheimer disease. *JAMA Neurol*, 71(11):1394, nov 2014.

[22] Mike A Nalls, Nathan Pankratz, Christina M Lill, Chuong B Do, Dena G Hernandez, Mohamad Saad, Anita L DeStefano, Eleanna Kara, Jose Bras, Manu Sharma, Claudia Schulte, Margaux F Keller, Sampath Arepalli, Christopher Letson, Connor Edsall, Hreinn Stefansson, Xinmin Liu, Hannah Pliner, Joseph H Lee, Rong Cheng, M Arfan Ikram, John P A Ioannidis, Georgios M Hadjigeorgiou, Joshua C Bis, Maria Martinez, Joel S Perlmutter, Alison Goate, Karen Marder, Brian Fiske, Margaret Sutherland, Georgia Xiromerisiou, Richard H Myers, Lorraine N Clark, Kari Stefansson, John A Hardy, Peter Heutink, Honglei Chen, Nicholas W Wood, Henry Houlden, Haydeh Payami, Alexis Brice, William K Scott, Thomas Gasser, Lars Bertram, Nicholas Eriksson, Tatiana Foroud, and Andrew B Singleton. Large-scale meta-analysis of genome-wide association data identifies six new risk loci for parkinson's disease. *Nat Genet*, 46(9):989–993, jul 2014.

[23] Gary H. Glover Paul Mazaika, Fumiko Hoeft and Allan L. Reiss. Methods and software for fmri analysis for clinical subjects. *Human Brain Mapping*, 2009.

[24] Francisco Pereira, Tom Mitchell, and Matthew Botvinick. Machine learning classifiers and fMRI: A tutorial overview. *NeuroImage*, 45(1):S199–S209, mar 2009.

[25] Sergey M. Plis, Devon R. Hjelm, Ruslan Salakhutdinov, Elena A. Allen, Henry J. Bockholt, Jeffrey D. Long, Hans J. Johnson, Jane S. Paulsen, Jessica A. Turner, and Vince D. Calhoun. Deep learning for neuroimaging: a validation study. *Frontiers in Neuroscience*, 8, aug 2014.

[26] Tamara Pringsheim, Katie Wiltshire, Lundy Day, Jonathan Dykeman, Thomas Steeves, and Nathalie Jette. The incidence and prevalence of Huntington's disease: a systematic review and meta-analysis. *Mov. Disord.*, 27(9):1083–1091, Aug 2012.

[27] J.-S. Provost, M. Petrides, F. Simard, and O. Monchi. Investigating the long-lasting residual effect of a set shift on frontostriatal activity. *Cerebral Cortex*, 22(12):2811–2819, 2012.

[28] Angela Rizk-Jackson, Diederick Stoffers, Sarah Sheldon, Josh Kuperman, Anders Dale, Jody Goldstein, Jody Corey-Bloom, Russell A. Poldrack, and Adam R. Aron. Evaluating imaging biomarkers for neurodegeneration in pre-symptomatic huntington's disease using machine learning techniques. *NeuroImage*, 56(2):788 – 796, 2011. Multivariate Decoding and Brain Reading.

[29] Bernhard Schölkopf and Alexander J Smola. *Learning with kernels: Support vector machines, regularization, optimization, and beyond*. MIT press, 2002.

[30] Jessica Schrouff, Maria Joao Rosa, Jane M Rondina, Andre F Marquand, Carlton Chu, John Ashburner, Christophe Phillips, Jonas Richiardi, and Janaina Mourão-Miranda. PRoNTo: pattern recognition for neuroimaging toolbox. *Neuroinformatics*, 11(3):319–337, Jul 2013.

[31] Alex J Smola and Bernhard Schölkopf. A tutorial on support vector regression. *Statistics and computing*, 14(3):199–222, 2004.

[32] Walker, Francis O. Huntington's disease. *The Lancet*, 369:218–228, 04 2015.

[33] V. Wottschel, D.C. Alexander, P.P. Kwok, D.T. Chard, M.L. Stromillo, N. De Stefano, A.J. Thompson, D.H. Miller, and O. Ciccarelli. Predicting outcome in clinically isolated syndrome using machine learning. *NeuroImage: Clinical*, 7:281–287, 2015.

[34] Mingjing Yang, Huiru Zheng, Haiying Wang, and Sally McClean. Feature selection and construction for the discrimination of neurodegenerative diseases based on gait analysis. In *Pervasive Computing Technologies for Healthcare, 2009. PervasiveHealth 2009. 3rd International Conference on*, pages 1–7, April 2009.

[35] Jonathan Young, Marc Modat, Manuel J. Cardoso, Alex Mendelson, Dave Cash, and Sebastien Ourselin. Accurate multimodal probabilistic prediction of conversion to alzheimer's disease in patients with mild cognitive impairment. *NeuroImage: Clinical*, 2(0):735 – 745, 2013.